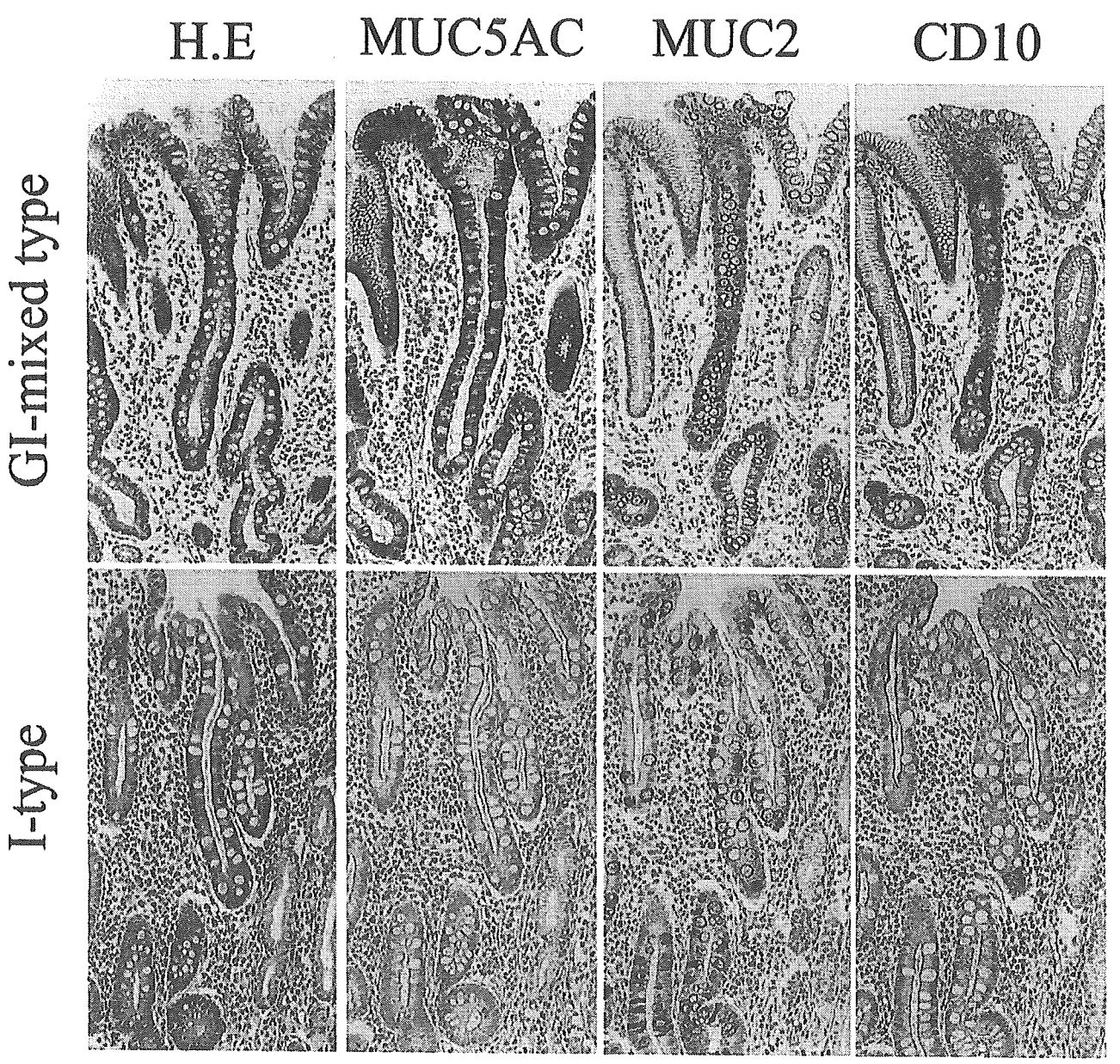

Figure 1 Immunnohistochemical analysis for IM glands with sequential sections. IM glands were detected by the expression of either CD10 or MUC2. Solely I-type IM glands express the intestinal markers without MUC5AC expression (lower panel, ×40), while GI-mixed-type IM glands express the intestinal markers with MUC5AC (upper panel, ×40).

apical end of MUC5AC-positive cells in GI-mixed-type IM glands, whose expressed cell numbers increased with diminishing MUC5AC expression in the glands. It is noteworthy that CD10 expression was not always detected with villin at the brush border in GI-mixed IM glands (Figure 6) but was also occasionally localized in the cytoplasm (Figure 5). Its inclusion body-like appearance was the same as that reported in familial microvillus-inclusion body disease (Groisman et al. 2002). This inclusion body-like CD10 staining pattern is more apparent in GI-mixed-type IM glands with more abundant MUC5AC-expressing cells, but it disappears with declining MUC5AC expression.

Discussion

To date, several immunohistochemical studies have demonstrated an intestinal or a gastric phenotype by the detection of specific molecular expressions in IM glands

The Journal of Histochemistry & Cytochemistry

The Journal of Histochemistry & Cytochemistry

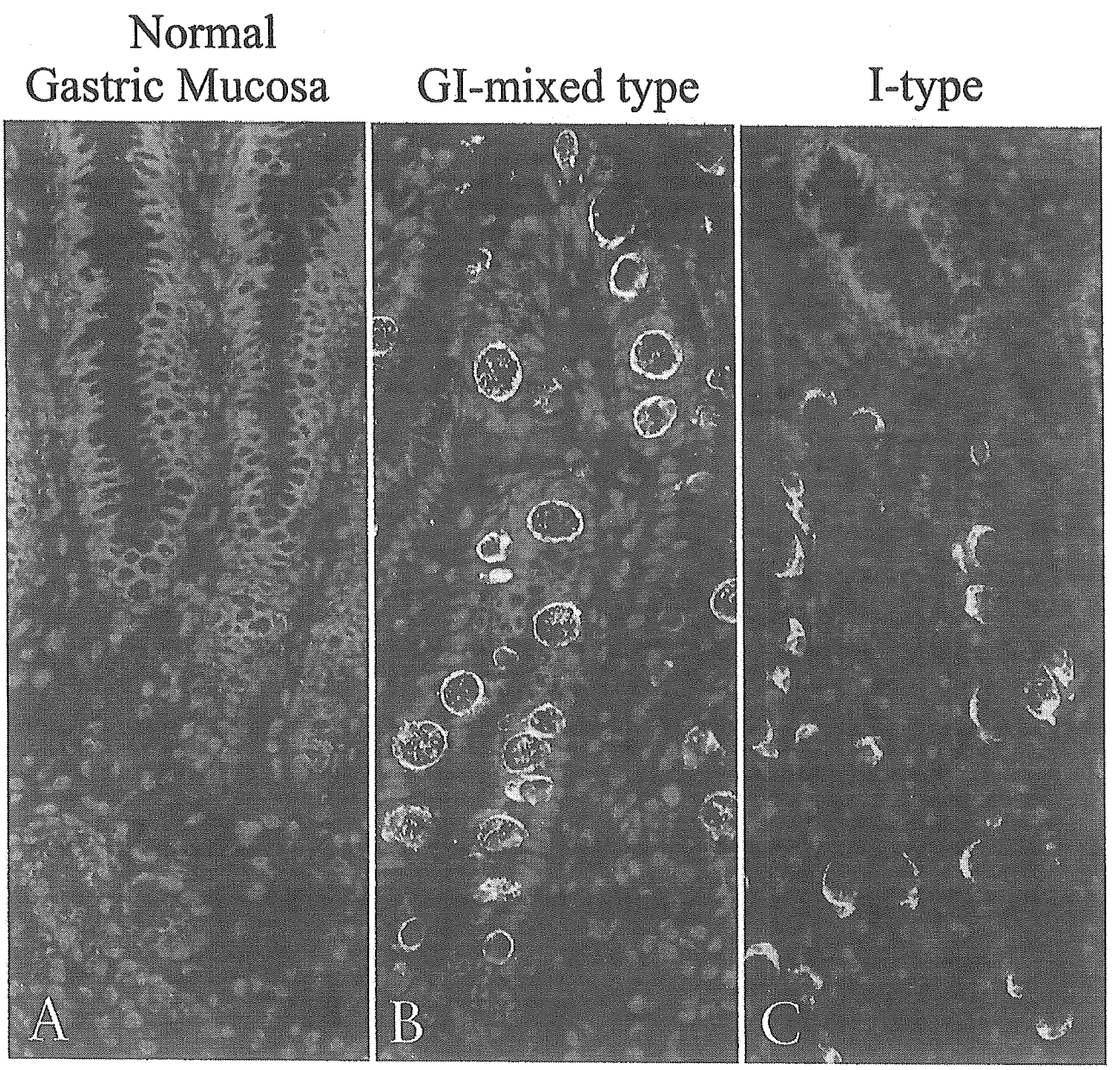

Figure 2 Localization of MUC5AC and MUC2 mucin core protein in normal gastric glands and IM glands. Frozen sections were stained with two mouse MAbs against MUC5AC directly labeled with AlexaFluor 568 and MUC2 with AlexaFluor 488 as described in Materials and Methods. Nuclei were counter-stained with DAPI (blue) and observed by fluorescence microscopy. MUC5AC (red) and MUC2 (green) mucin core protein expressions were observed in the cytoplasm of foveolar epithelial cells in normal gastric mucosa (**A**) and in the Golgi apparatus of goblet cells in solely I-type IM glands (**C**), respectively. Colocalization of MUC5AC and MUC2 on the same cells was demonstrated by merged images (yellow) in GI-mixed-type IM glands (**B**, ×60).

using serial sections (Ho et al. 1995; Inada et al. 1997, 2001; Reis et al. 1999; Jass 2000; Shaoul et al. 2000; Silva et al. 2002; Tatematsu et al. 2003). These studies have attempted to demonstrate that some cells are either intestinal or gastric phenotypic markers, suggesting limited possibilities for the same cells to have both gastric- and intestinal-marker antigens (Reis et al. 1999, 2000; Lopez-Ferrer et al. 2000,2001; Shaoul et al. 2000). In the present study, we were able to overcome such limitations by employing Zenon antibody-labeling technology, thus successfully demonstrating the co-expression of both gastric and intestinal molecular markers in the same cells in GI-mixed-type IM glands, in which MUC5AC clearly existed with MUC2, or vil-

The Journal of Histochemistry & Cytochemistry

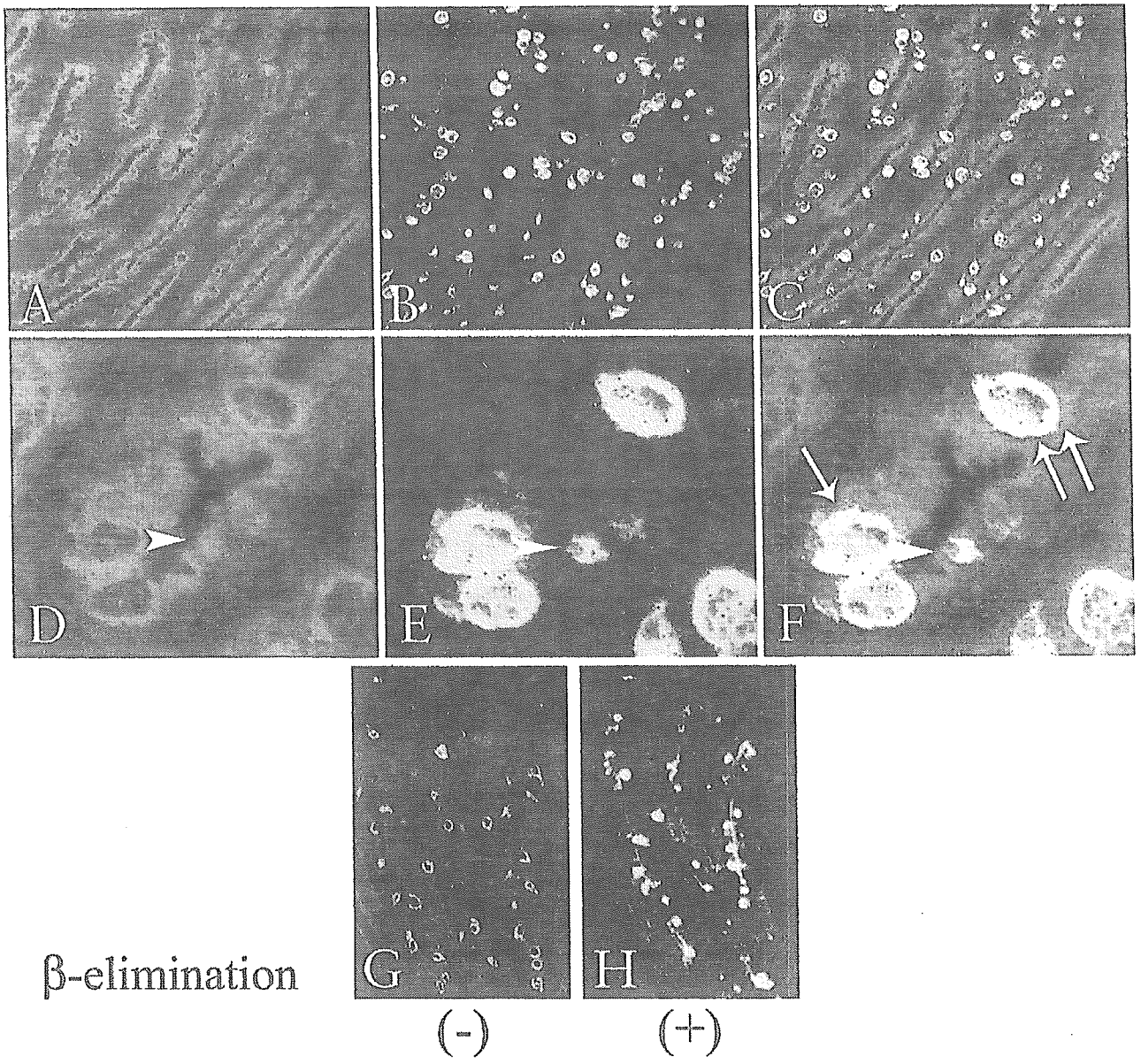

Figure 3 Colocalization of MUC5AC and MUC2 mucin core proteins in GI-mixed-type IM glands. Frozen sections were stained by the double-immunofluorescence method using two mouse MAbs against MUC5AC and MUC2 directly labeled with AlexaFluor 568 or 488. MUC5AC (red) and MUC2 (green) expressions in GI-mixed-type IM glands were observed by confocal laser scanning microscopy (**A–C**: low-power views; **D–F**: high-power views). **(A,D)** MUC5AC was observed in the cytoplasm of almost all columnar epithelial and goblet cells, except for the center of a secretory vesicle of goblet cells. **(B,E)** MUC2 expressions were observed in the Golgi area in columnar cells (arrowhead) and the secretory vesicles in goblet cells. **(C,F)** Colocalization of MUC5AC and MUC2 was seen on the periphery of secretory vesicles in the composite images (yellow, arrow). **(G,H)** β-elimination increased MUC2 antibody (Ccp58) reactivity in mucous vesicle of solely I-type IM glands. **(A–C,G,H** ×20), **(D–F,** ×60).

lin and/or CD10. These findings suggest that mixed gastric and intestinal type metaplasia is formed by cells with dual differentiation and are consistent with the previously demonstrated evidence that some metaplastic cells have both intestinal and gastric differentiation-specific structures (Goldman and Ming 1968).

The cells in GI-mixed-type IM glands exhibited MUC2 with MUC5AC in their cytoplasm (Figures 2 and 3), while the cells in I-type IM glands exhibited MUC2 in the peri-nuclear Golgi apparatus area. The subcellular localization of MUC2 appeared to shift from secretion vesicles to the Golgi apparatus area with a

The Journal of Histochemistry & Cytochemistry

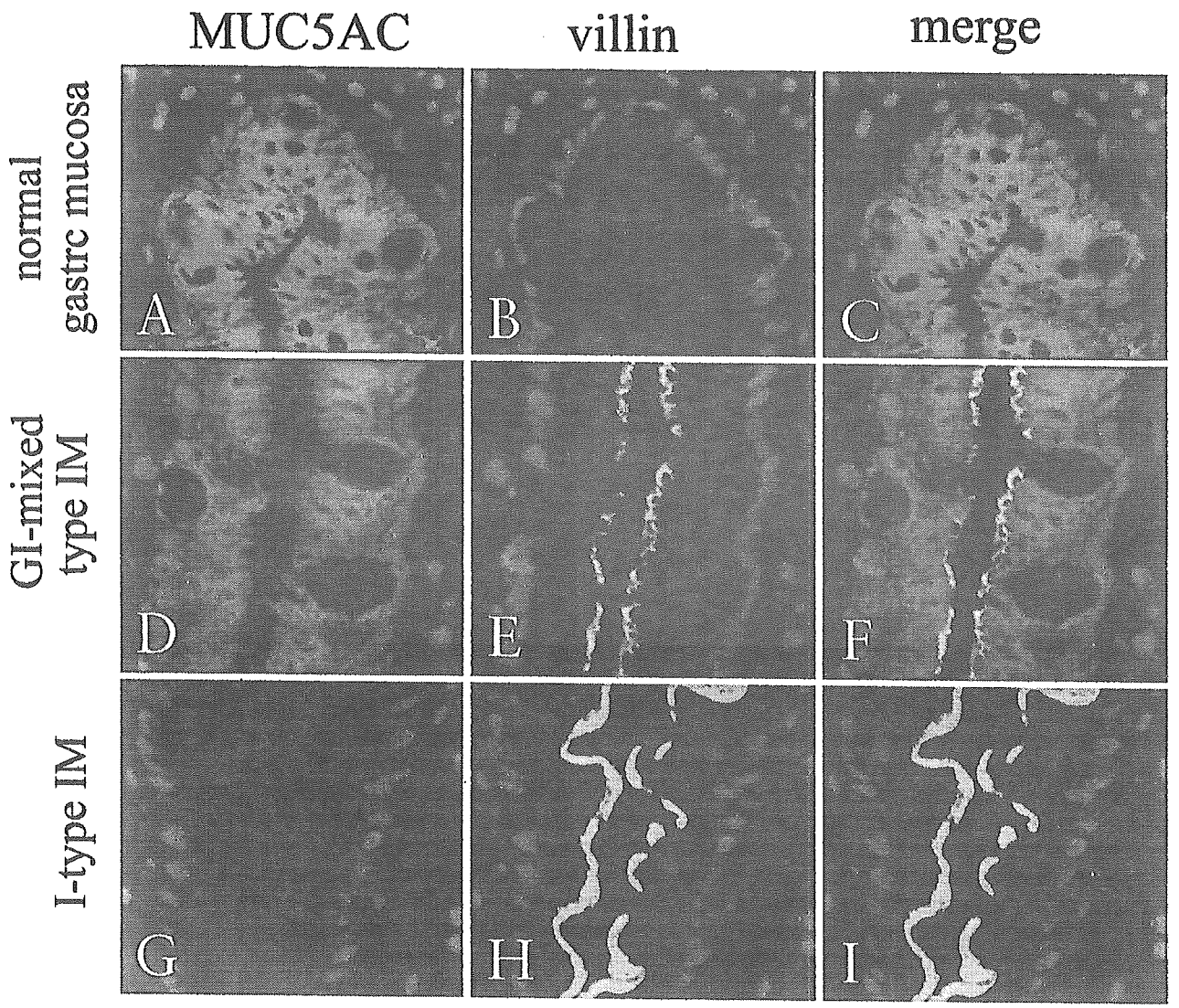

Figure 4 Expression of MUC5AC and villin in normal gastric glands and GI-mixed-type IM glands. Frozen sections were stained by the double-immunofluorescence method using two mouse MAbs against villin and MUC5AC directly labeled with AlexaFluor 488 or 568. Nuclei were counter-stained by DAPI (blue) and observed by fluorescence microscopy. **(A–C)** Only MUC5AC (red) without villin (green) was seen in gastric columnar epithelial cells. **(G–I)** Such cells in I-type IM glands exhibited only villin without MUC5AC. **(D–F)** MUC5AC was observed in the cytoplasm and villin of the micro-villi of the columnar cells in GI-mixed-type IM glands. Composite images demonstrate the absence of any yellow signal in the cells, suggesting their different subcellular localization **(F)**. **(A–I,** ×60**)**.

histological alteration from GI-mixed-type IM to I-type IM. A glycosylation change might be one of the probable explanations, since the MUC 2 antibody used in this study could detect only underglycosylated MUC2 core protein for the epitope as discussed in previous studies (Hong and Kim 2000; Shaoul et al. 2000). In the present study we observed the enhanced anti-MUC2 antibody staining in I-type IM glands by alkali-catalyzed β-elimination, which was similar to the MUC2 staining on GI-mixed-type IM glands. This result indicates that O-linked glycosylation limited the detection of MUC2 expression in goblet cells in I-type IM glands, suggesting that the difference between the higher glycosylated MUC2 in I-type IM glands and the lower glycosylated MUC2 in the goblet cells in the GI-mixed-type IM glands would be the other maturation indicator for goblet cells in IM glands.

The columnar epithelial cells, similar to the intestinal absorptive cells, were seen in GI-mixed-type IM glands that exhibited MUC5AC and either villin or CD10. Compared with villin-positive cells, CD10 was preferentially found in the faint MUC5AC-preserved columnar cells, suggesting that CD10 exists in cells of the more intestinalized GI-mixed-type IM glands (Fig-

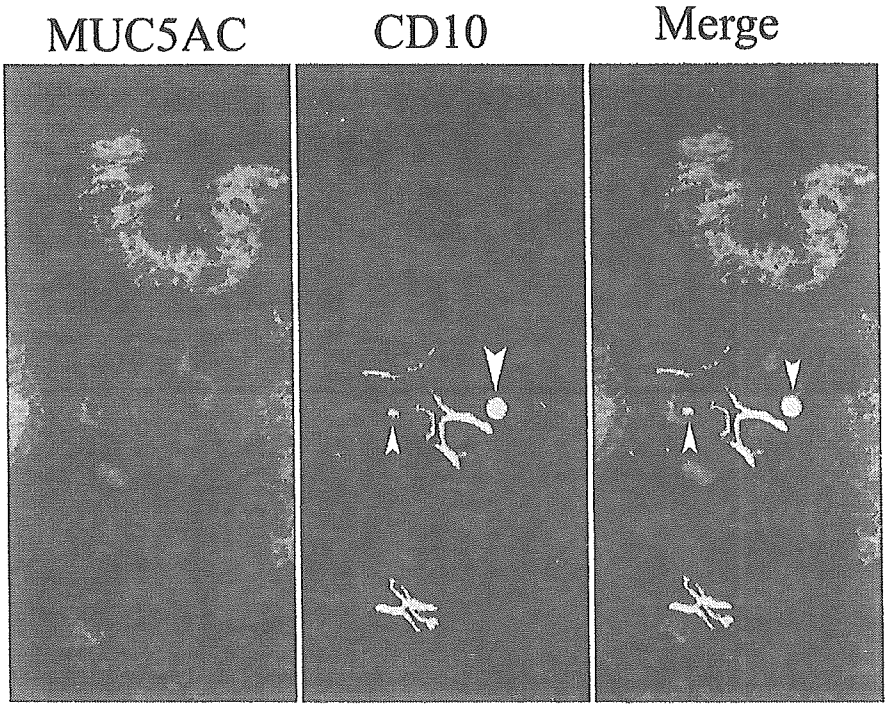

Figure 5 Cellular localization of CD10 in GI-mixed IM glands. Frozen sections were stained by the double-immunofluorescence method using two mouse MAbs against MUC5AC and CD10 directly labeled with AlexaFluor 568 and 488, respectively. This figure was obtained by fluorescence microscopy. CD10 (green) was expressed in the microvilli of columnar cells without MUC5AC expression (red), while CD10 stained as inclusion body-like signals in MUC5AC-positive cells. Arrowheads indicate CD10-positive inclusion bodies (×60).

ure 6). Analogously, in the development of fetal mouse small intestine, villin appears on the brush border prior to CD10 (Landry et al. 1994; Montgomery et al. 1999). Villin is an actin-binding cytoskeletal protein essential for brush border formation in normal epithelial cells of the intestine, while CD10 is a brush border-associated neutral peptidase. Adapting these findings to human IM, the structural accomplishment of IMs such as villin expression might precede by functional maturations such as digestive enzyme, CD10 expression. Moreover, it may be reasonable to assume that villin-positive and CD10-negative cells in GI-mixed-type IM are functionally immature absorptive cells, and that the phenotype shift from GI-mixed-type IM to solely I-type IM is a kind of maturation. Furthermore, the expression of CD10 in the cytoplasm of columnar cells in GI-mixed IM (Figure 5) might support this idea, because it has been found in the surface enterocytes of familial microvillus inclusion disease due to the immaturity of CD10 (Groisman et al. 2002).

Co-expression ratios of MUC5AC to MUC2, villin, or CD10 varied greatly in terms of establishing a dominant MUC5AC type or a MUC2/villin/CD10 dominant type. Based on these findings, the cells in mixed-type IM glands seem to be about to free themselves from the gastric phenotype, finally becoming solely I-type IM cells. As villin, CD10, and MUC2 expressions progressively increase, MUC5AC expression reciprocally diminishes. Gastric-type cells are gradually reduced and finally replaced by intestinal-type cells, leading to solely I-type IM. These results indicate that GI-mixed-type IM cells are multi-phenotypic, suggesting that the phenotype shift from a GI-mixed type to a solely I-type IM should occur in each cell over time (Figure 7).

In conclusion, we demonstrated that intestinalization occurs in individual cells with MUC5AC expression in GI-mixed-type IM glands. The cells with an intestinal phenotype in GI-mixed type IM glands are morphologically and functionally less mature than those in I-type IM glands. As they are midway between gastric and intestinal phenotypic cells with varying degrees of differentiation and maturation, the GI-mixed-type IM glands consist of a heterogeneous population of cells. Based on observations in this study, we hypothesize that the cells in GI-mixed-type IM glands remain out of some regulations on intestinal differentiation and subsequent functional maturation toward becoming intestinal type cells. Furthermore, considering that stem cells are also present in GI-mixed-type IM, such unstable phenotypes might be induced at stem cells by either transcriptional factors or DNA methylation. To clarify and confirm these possibilities, further studies based on molecular biological techniques and applying our findings will have to be initiated starting with the identification of GI-mixed IM cells.

Acknowledgments

Supported by a Grant-in-Aid for Scientific Research on Priority Area (16790196) from the Ministry of Education, Culture, Sports, Science and Technology of Japan.

The Journal of Histochemistry & Cytochemistry

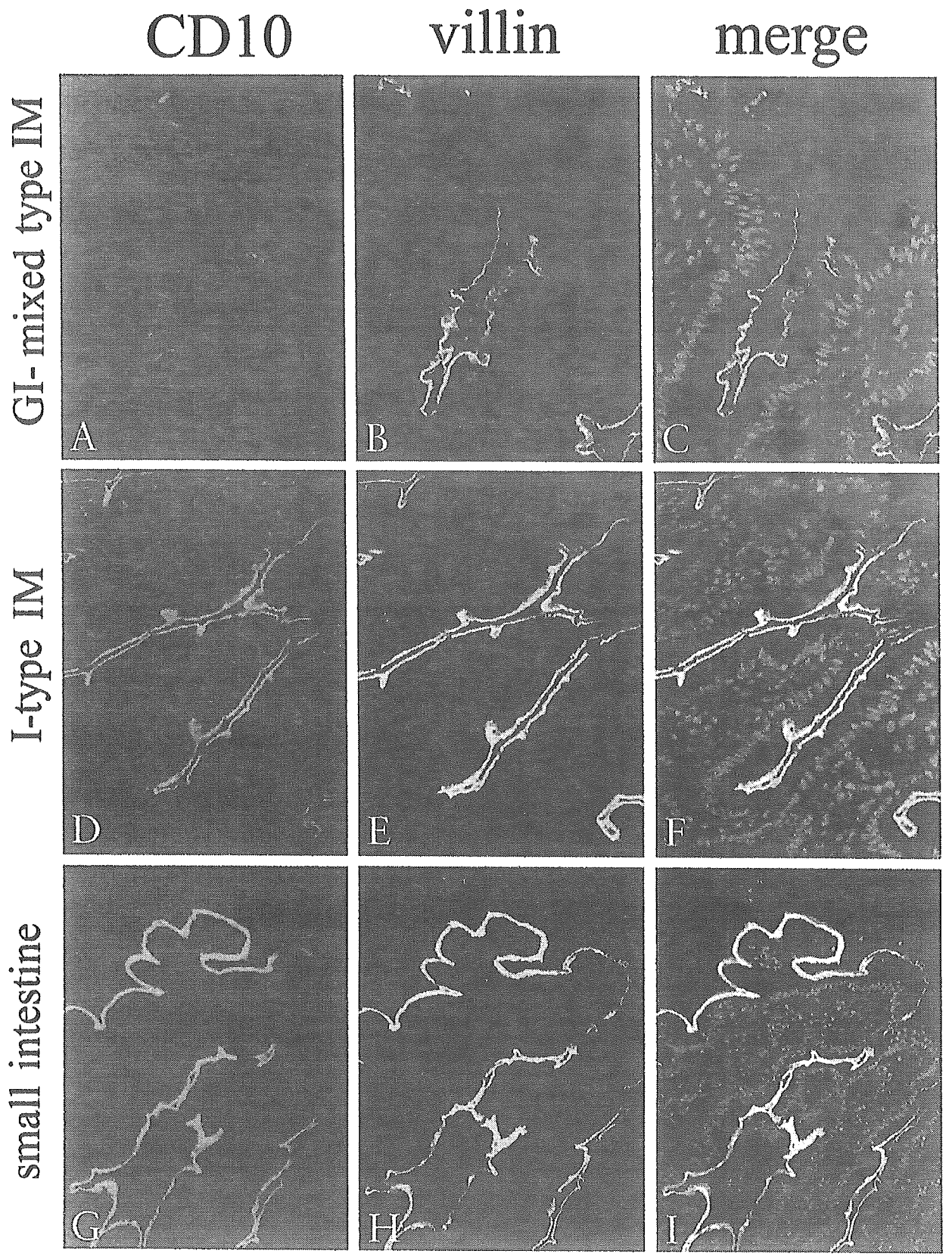

Figure 6 Expression of villin and CD10 in GI-mixed IM glands. Frozen sections were stained by the double-immunofluorescent method using two mouse MAbs against villin and CD10 directly labeled with AlexaFluor 488 and 568, respectively. Nuclei were counter-stained by DAPI (blue) and observed by fluorescence microscopy. CD10 (red; **A,D,G**) and villin (green; **B,E,H**) were observed to be colocalized in the micro-villi of columnar cells in I-type IM glands and small intestine by composite images (yellow) (**F,I**). In contrast, compared with villin (**B**), CD10 expression (**A**) was faint in GI-mixed-type IM glands, and the colocalization was barely visible (**C**). (**A–I**, ×20).

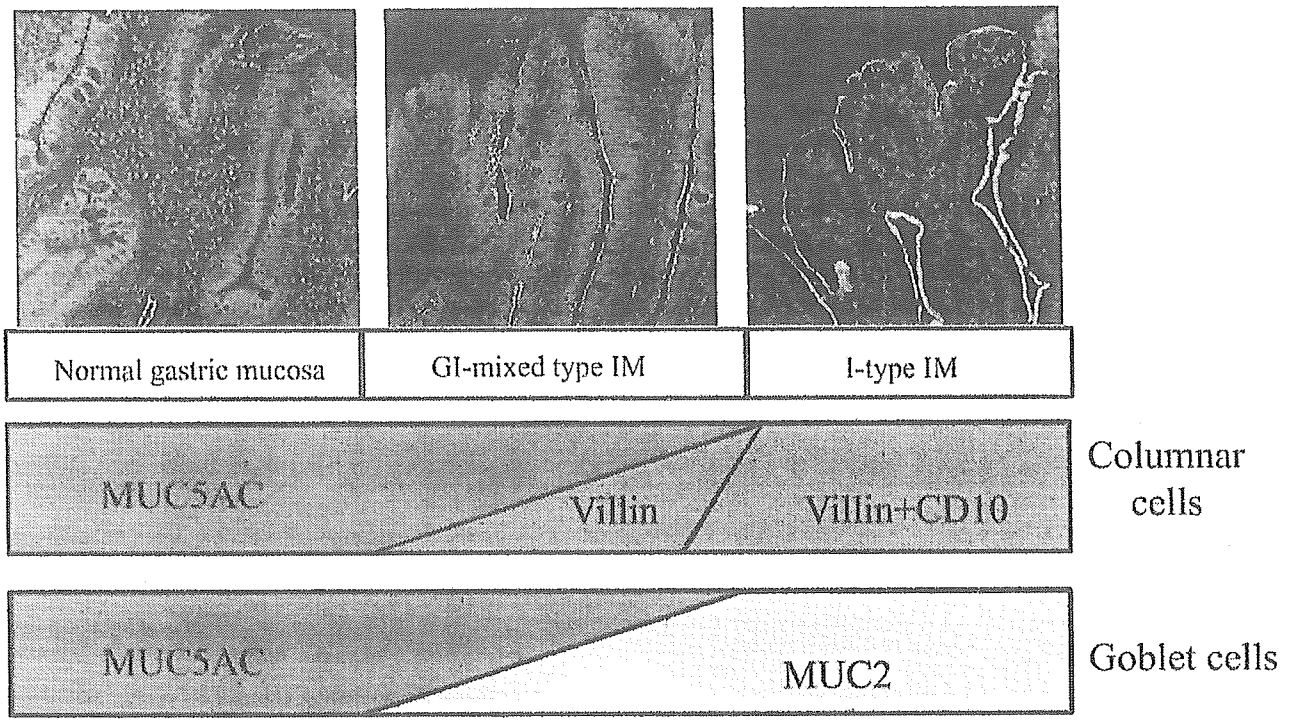

Figure 7 Schematic representation of phenotypic shift of differentiation markers from GI-mixed-type IM to I-type IM glands. Gastric foveolar epithelial cells express only MUC5AC. IM begins from such foveolar epithelial cells, along two different cellular pathways. One begins with an aberrant expression of villin and subsequent CD10 on columnar epithelial cells, resulting in absorptive-like intestinal cells. The other starts from an ectopic expression of MUC2 and then accumulates in mucous vesicles, developing into goblet-like intestinal cells. As villin, CD10, and MUC2 expressions progressively increase, MUC5AC expression reciprocally diminishes. Gastric-type cells are gradually reduced and are finally replaced by intestinal-type cells, leading to solely I-type IM (upper panel, ×20).

Literature Cited

Chen Y, Zhao YH, Kalaslavadi TB, Hamati E, Nehrke K, Le AD, Ann DK, Wu R (2003) Genome-wide search and identification of a novel gel-forming mucin MUC19/Muc19 in glandular tissues. Am J Respir Cell Mol Biol 30:155–165

Correa P (1992) Human gastric carcinogenesis: a multistep and multifactorial process—First American Cancer Society Award Lecture on Cancer Epidemiology and Prevention. Cancer Res 52: 6735–6740

Filipe MI, Barbatis C, Sandey A, Ma J (1988) Expression of intestinal mucin antigens in the gastric epithelium and its relationship with malignancy. Hum Pathol 19:19–26

Filipe MI, Potet F, Bogomoletz WV, Dawson PA, Fabiani B, Chauveinc P, Fenzy A, Gazzard B, Goldfain D, Zeegen R (1985) Incomplete sulphomucin-secreting intestinal metaplasia for gastric cancer. Preliminary data from a prospective study from three centres. Gut 26:1319–1326

Goldman H, Ming SC (1968) Fine structure of intestinal metaplasia and adenocarcinoma of the human stomach. Lab Invest 18:203–210

Groisman GM, Amar M, Livne E (2002) CD10: a valuable tool for the light microscopic diagnosis of microvillous inclusion disease (familial microvillous atrophy). Am J Surg Pathol 26:902–907

Gum JR Jr, Crawley SC, Hicks JW, Szymkowski DE, Kim YS (2002) MUC17, a novel membrane-tethered mucin. Biochem Biophys Res Commun 291:466–475

Ho SB, Shekels LL, Toribara NW, Kim YS, Lyftogt C, Cherwitz DL, Niehans GA (1995) Mucin gene expression in normal, preneoplastic, and neoplastic human gastric epithelium. Cancer Res 55:2681–2690

Hong JC, Kim YS (2000) Alkali-catalyzed beta-elimination of periodate-oxidized glycans: a novel method of chemical deglycosylation of mucin gene products in paraffin embedded sections. Glycoconj J 17:691–703

Inada K, Nakanishi H, Fujimitsu Y, Shimizu N, Ichinose M, Miki K, Nakamura S, Tatematsu M (1997) Gastric and intestinal mixed and solely intestinal types of intestinal metaplasia in the human stomach. Pathol Int 47:831–841

Inada K, Tanaka H, Nakanishi H, Tsukamoto T, Ikehara Y, Tatematsu K, Nakamura S, Porter EM, Tatematsu M (2001) Identification of Paneth cells in pyloric glands associated with gastric and intestinal mixed-type intestinal metaplasia of the human stomach. Virchows Arch 439:14–20

Jass JR (2000) Mucin core proteins as differentiation markers in the gastrointestinal tract. Histopathology 37:561–564

Jass JR, Filipe MI (1979) A variant of intestinal metaplasia associated with gastric carcinoma: a histochemical study. Histopathology 3:191–199

Jass JR, Walsh MD (2001) Altered mucin expression in the gastrointestinal tract: a review. J Cell Mol Med 5:327–351

Kang GH, Lee HJ, Hwang KS, Lee S, Kim JH, Kim JS (2003a) Aberrant CpG island hypermethylation of chronic gastritis, in relation to aging, gender, intestinal metaplasia, and chronic inflammation. Am J Pathol 163:1551–1556

Kang GH, Lee S, Kim JS, Jung HY (2003b) Profile of aberrant CpG island methylation along the multistep pathway of gastric carcinogenesis. Lab Invest 83:635–641

Kang GH, Shim YH, Jung HY, Kim WH, Ro JY, Rhyu MG (2001) CpG island methylation in premalignant stages of gastric carcinoma. Cancer Res 61:2847–2851

Kawachi H, Takizawa T, Eishi Y, Shimizu S, Kumagai J, Funata N,

The Journal of Histochemistry & Cytochemistry

Koike M (2003) Absence of either gastric or intestinal phenotype in microscopic differentiated gastric carcinomas. J Pathol 199: 436–446

Kawachi T, Kogure K, Tanaka N, Tokunaga A, Sugimura T (1974) Studies of intestinal metaplasia in the gastric mucosa by detection of disaccharidases with "Tes-Tape". J Natl Cancer Inst 53:19–30

Kim TY, Lee HJ, Hwang KS, Lee M, Kim JW, Bang YJ, Kang GH (2004) Methylation of RUNX3 in various types of human cancers and premalignant stages of gastric carcinoma. Lab Invest 84: 479–484

Landry C, Huet C, Mangeat P, Sahuquet A, Louvard D, Crine P (1994) Comparative analysis of neutral endopeptidase (NEP) and villin gene expression during mouse embryogenesis and enterocyte maturation. Differentiation 56:55–65

Lee JH, Park SJ, Abraham SC, Seo JS, Nam JH, Choi C, Juhng SW, Rashid A, Hamilton SR, Wu TT (2004) Frequent CpG island methylation in precursor lesions and early gastric adenocarcinomas. Oncogene 23:4646–4654

Lopez-Ferrer A, Barranco C, de Bolos C (2001) Apomucin expression and association with Lewis antigens during gastric development. Appl Immunohistochem Mol Morphol 9:42–48

Lopez-Ferrer A, de Bolos C, Barranco C, Garrido M, Isern J, Carlstedt I, Reis CA, Torrado J, Real FX (2000) Role of fucosyltransferases in the association between apomucin and Lewis antigen expression in normal and malignant gastric epithelium. Gut 47: 349–356

MacLennan AJ, Orringer MB, Beer DG (1999) Identification of intestinal-type Barrett's metaplasia by using the intestine-specific protein villin and esophageal brush cytology. Mol Carcinog 24: 137–143

Matsukuma A, Mori M, Enjoji M (1990) Sulphomucin-secreting intestinal metaplasia in the human gastric mucosa. An association with intestinal-type gastric carcinoma. Cancer 66:689–694

Matsukura N, Suzuki K, Kawachi T, Aoyagi M, Sugimura T, Kitaoka H, Numajiri H, Shirota A, Itabashi M, Hirota T (1980) Distribution of marker enzymes and mucin in intestinal metaplasia in human stomach and relation to complete and incomplete types of intestinal metaplasia to minute gastric carcinomas. J Natl Cancer Inst 65:231–240

Mizoshita T, Inada K, Tsukamoto T, Kodera Y, Yamamura Y, Hirai T, Kato T, Joh T, Itoh M, Tatematsu M (2001) Expression of Cdx1 and Cdx2 mRNAs and relevance of this expression to differentiation in human gastrointestinal mucosa–with special emphasis on participation in intestinal metaplasia of the human stomach. Gastric Cancer 4:185–191

Montgomery RK, Mulberg AE, Grand RJ (1999) Development of the human gastrointestinal tract: twenty years of progress. Gastroenterology 116:702–731

Morson BC (1955) Carcinoma arising from areas of intestinal metaplasia in the gastric mucosa. Br J Cancer 9:377–385

Pigny P, Guyonnet-Duperat V, Hill AS, Pratt WS, Galiegue-Zouitina S, d'Hooge MC, Laine A, Van-Seuningen I, Degand P, Gum JR, Kim YS, Swallow DM, Aubert JP, Porchet N (1996) Human mucin genes assigned to 11p15.5: identification and organization of a cluster of genes. Genomics 38:340–352

Pinto D, Robine S, Jaisser F, El Marjou FE, Louvard D (1999) Cells of small and large intestines. J Biol Chem 274:6476–6482 Regulatory sequences of the mouse villin gene that efficiently drive transgenic expression in immature and differentiated epithelial cells of small and large intestines. J Biol Chem 274:6476–6482

Reis CA, David L, Carvalho F, Mandel U, de Bolos C, Mirgorodskaya E, Clausen H, Sobrinho-Simoes M (2000) Immunohistochemical study of the expression of MUC6 mucin and co-expression of other secreted mucins (MUC5AC and MUC2) in human gastric carcinomas. J Histochem Cytochem 48:377–388

Reis CA, David L, Correa P, Carneiro F, de Bolos C, Garcia E, Mandel U, Clausen H, Sobrinho-Simoes M (1999) Intestinal metaplasia of human stomach displays distinct patterns of mucin (MUC1, MUC2, MUC5AC, and MUC6) expression. Cancer Res 59:1003–1007

Reis CA, David L, Nielsen PA, Clausen H, Mirgorodskaya K, Roepstorff P, Sobrinho-Simoes M (1997) Immunohistochemical study of MUC5AC expression in human gastric carcinomas using a novel monoclonal antibody. Int J Cancer 74:112–121

Ringel J, Lohr M (2003) The MUC gene family: their role in diagnosis and early detection of pancreatic cancer. Mol Cancer 2:9

Segura DI, Montero C (1983) Histochemical characterization of different types of intestinal metaplasia in gastric mucosa. Cancer 52:498–503

Sezaki N, Ishimaru F, Tabayashi T, Kataoka I, Nakase K, Fujii K, Kozuka T, Nakayama H, Harada M, Tanimoto M (2003) The type 1 CD10/neutral endopeptidase 24.11 promoter: functional characterization of the 5′-untranslated region. Br J Haematol 123:177–183

Shaoul R, Marcon P, Okada Y, Cutz E, Forstner G (2000) The pathogenesis of duodenal gastric metaplasia: the role of local goblet cell transformation. Gut 46:632–638

Silberg DG, Furth EE, Taylor JK, Schuck T, Chiou T, Traber PG (1997) CDX1 protein expression in normal, metaplastic, and neoplastic human alimentary tract epithelium. Gastroenterology 113:478–486

Silberg DG, Sullivan J, Kang E, Swain GP, Moffett J, Sund NJ, Sackett SD, Kaestner KH (2002) Cdx2 ectopic expression induces gastric intestinal metaplasia in transgenic mice. Gastroenterology 122:689–696

Silva E, Teixeira A, David L, Carneiro F, Reis CA, Sobrinho-Simoes J, Serpa J, Veerman E, Bolscher J, Sobrinho-Simoes M (2002) Mucins as key molecules for the classification of intestinal metaplasia of the stomach. Virchows Arch 440:311–317

Stemmermann GN, Hayashi T (1968) Intestinal metaplasia of the gastric mucosa: a gross and microscopic study of its distribution in various disease states. J Natl Cancer Inst 41:627–634

Sugimura T, Matsukura N, Sato S (1982) Intestinal metaplasia of the stomach as a precancerous stage. IARC Sci Publ 39:515–530

Tanaka H, Matsui T, Agata A, Tomura M, Kubota I, McFarland KC, Kohr B, Lee A, Phillips HS, Shelton DL (1991) Molecular cloning and expression of a novel adhesion molecule, SC1. Neuron 7:535–545

Tatematsu M, Tsukamoto T, Inada K (2003) Stem cells and gastric cancer: role of gastric and intestinal mixed intestinal metaplasia. Cancer Sci 94:135–141

Teglbjaerg PS, Nielsen HO (1978) "Small intestinal type" and "colonic type" intestinal metaplasia of the human stomach, and their relationship to the histogenetic types of gastric adenocarcinoma. Acta Pathol Microbiol Scand [A] 86A:351–355

Tsukamoto T, Inada K, Tanaka H, Mizoshita T, Mihara M, Ushijima T, Yamamura Y, Nakamura S, Tatematsu M (2003) Down-regulation of a gastric transcription factor, Sox2, and ectopic expression of intestinal homeobox genes, Cdx1 nd Cdx2: inverse correlation during progression from gastric/intestinal-mixed to complete intestinal metaplasia. J Cancer Res Clin Oncol 130: 135–145

Winterford CM, Walsh MD, Leggett BA, Jass JR (1999) Ultrastructural localization of epithelial mucin core proteins in colorectal tissues. J Histochem Cytochem 47:1063–1074

You WC, Blot WJ, Li JY, Chang YS, Jin ML, Kneller R, Zhang L, et al. (1993) Precancerous gastric lesions in a population at high risk of stomach cancer. Cancer Res 53:1317–1321

Yuasa Y (2003) Control of gut differentiation and intestinal-type gastric carcinogenesis. Nat Rev Cancer 3:592–600

The Journal of Histochemistry & Cytochemistry

Contrast Harmonic Sonographically Guided Radio Frequency Ablation for Spontaneous Ruptured Hepatocellular Carcinoma

Hideyuki Tamai, MD, Masashi Oka, MD, Hiroki Maeda, MD, Naoki Shingaki, MD, Takayuki Kanno, MD, Shotaro Enomoto, MD, Tatuya Shiraki, MD, Mikitaka Iguchi, MD, Kazuyuki Nakazawa, MD, Kenji Arii, MD, Kimihiko Yanaoka, MD, Yasuhito Shimizu, MD, Hiroya Nakata, MD, Mitsuhiro Fujishiro, MD, Naohisa Yahagi, MD, Shuichiro Shiina, MD, Masao Ichinose, MD

Intraperitoneal bleeding due to a ruptured tumor is a serious complication in patients with hepatocellular carcinoma (HCC). According to data compiled by the Liver Cancer Study Group of Japan,[1] ruptured HCC accounts for around 10% of deaths in these patients. Clinical features include the sudden onset of abdominal pain and distension and, if bleeding is massive, the presence of shock. Other causes of an acute abdominal emergency must be ruled out. Diagnostic imaging generally includes sonography, contrast computed tomography (CT), and angiography. In patients with ruptured HCC, prompt diagnosis and treatment is essential to avoid hepatocyte necrosis and secondary hepatic failure associated with shock and decreased hepatic perfusion due to bleeding.

The underlying liver disease varies in such patients with ruptured HCC. Chronic hepatitis, cirrhosis, or both may be present, and the severity of hepatic dysfunction as well as the size, number, and progression of the neoplastic lesions present varies from case to case. A common feature is the presence of a responsible lesion on or protruding from the surface of the liver. If hemostasis can be achieved early after HCC rupture, then overall prognosis depends on the patient's liver function and degree of tumor progression. Although there is a risk of intraperitoneal seeding, long-term survival is possible if the tumor can be completely resected by hepatectomy. One study has already reported a good 5-year survival rate after resection of ruptured and nonruptured HCC.[2] In another study, rather than performing emergency surgery, Marini et al[3] used transcatheter arterial embolization (TAE) to control bleeding; in those patients who could then undergo surgery, elective hepatectomy was associated with long-term survival. Treatment of ruptured HCC involves more than just hemostasis. Subsequent therapy is important, and, whenever possible, complete resection should be performed after bleeding has been controlled.

Abbreviations
CT, computed tomography; HCC, hepatocellular carcinoma; PEIT, percutaneous ethanol injection therapy; RFA, radio frequency ablation; S, segment; TAE, transcatheter arterial embolization

Received January 19, 2005, from the Second Department of Internal Medicine, Wakayama Medical University, Wakayama, Japan (H.T., M.O., H.M., N.S., T.K., S.E., T.S., M.I., K.N., K.A., K.Y., Y.S., H.N., M.I.); and Department of Gastroenterology, University of Tokyo, Tokyo, Japan (M.F., N.Y., S.S.). Revision requested February 7, 2005. Revised manuscript accepted for publication March 1, 2005.

Address correspondence to Hideyuki Tamai, MD, Second Department of Internal Medicine, Wakayama Medical University, 811-1 Kimiidera, Wakayama City, Wakayama 640-0012, Japan.

© 2005 by the American Institute of Ultrasound in Medicine • J Ultrasound Med 2005; 24:1021–1026 • 0278-4297/05/$3.50

Nevertheless, in a series of 172 patients with ruptured HCC in Japan, Miyamoto et al[4] reported that subsequent hepatectomy was possible in only 12% of cases; in most cases, the presence of multiple lesions or underlying cirrhosis made surgery difficult. In patients in whom hepatectomy cannot be performed, relatively radical yet less invasive treatment with percutaneous radio frequency ablation (RFA) may lead to an improved prognosis.

Transcatheter arterial embolization is now widely used as first-line treatment to achieve safe and reliable hemostasis in ruptured HCC. However, extensive TAE may worsen liver function and lead to post-TAE hepatic failure. In addition, angiographic localization of the bleeding site in ruptured HCC is difficult and is successful in 20% of cases at most.[5] Accurate localization of the bleeding site allows for hemostasis with superselective TAE and local ablative therapy that can minimize injury to nontumor tissue and reduce the risk of posttreatment hepatic failure. In the case of ruptured HCC reported here, we identified the site of bleeding by contrast harmonic sonography and performed RFA under sonographic guidance to achieve hemostasis. This case shows the successful application of percutaneous ablative therapy guided by contrast harmonic sonography.

Case Report

The patient was a 56-year-old man who had been followed for chronic hepatitis C at our outpatient clinic since 1992. In June 1999, hepatomas involving Couinaud segment 7 (S7; 18 mm in diameter) and S8 (25 mm) were found and were subsequently treated with TAE and percutaneous ethanol injection therapy (PEIT). In 2001, local recurrence as well as recurrence at other hepatic sites was noted, and RFA was performed. Eight months later, the patient had abdominal pain and distension and was hospitalized after consulting our clinic 2 days later. The only episode of note in the medical history was appendectomy at age 15 years; blood transfusion was required during that admission. The family history was notable in that both parents and an older brother had died of HCC. The patient also reported a 35-year history of alcohol consumption (≈0.54 L of sake, Japanese rice wine, per day). At admission, the patient was lucid and afebrile, and physical examination revealed pallor and tachycardia with no sign of shock (blood pressure, 120/60 mm Hg; pulse rate, 124 beats per minute, regular). Jaundice and ascites were apparent, but peripheral edema was not. The hemoglobin concentration was 10.6 g/dL. Liver function was severely impaired, with a total bilirubin level of 3.2 mg/dL, an albumin level of 2.6 g/dL, and prothrombin time of 36.2%. Serum aspartate aminotransferase and alanine aminotransferase levels were markedly elevated at 825 and 353 IU/L, respectively. α-Fetoprotein (106.0 ng/mL), lens culinaris agglutinin-reactive α-fetoprotein (12.9%), and des-γ-carboxy prothrombin (241 milli-arbitrary units/mL) levels were also elevated, indicating a recurrence of HCC. Abdominal

Figure 1. Abdominal contrast CT. **A**, An irregular low-density mass in S7 and S8 indicates scarring from previously treated HCC, but a new 3-cm tumor is also present on the S2 liver surface (arrow). During the arterial phase, no contrast enhancement is observed. **B**, During the equilibrium phase, the tumor has low density (arrow). A large amount of ascites is present, but no areas of high density suggesting blood clots and no leakage of contrast material are shown.

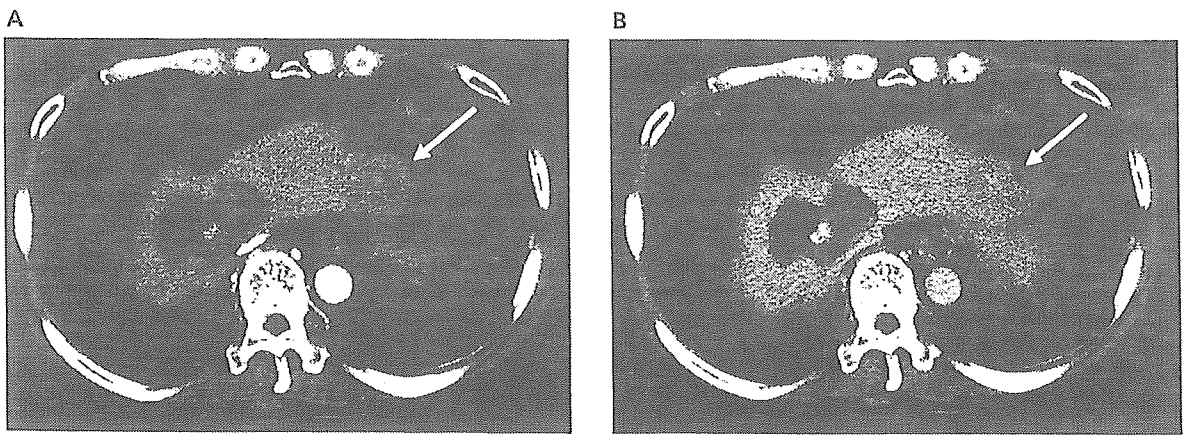

contrast CT showed a large volume of ascites present in the peritoneal cavity but no areas of high density suggestive of hematoma or leakage of contrast into the peritoneum (Figure 1). Several posttreatment nodules were evident in the right lobe of the liver, and a new 3-cm tumor was observed on the surface of S2. No enhancement occurred during the arterial phase, and the lesion was hypodense during the equilibrium phase. Although there was no sign of intraperitoneal hemorrhage, as abdominal paracentesis revealed grossly hemorrhagic fluid, we considered a diagnosis of ruptured HCC to be highly probable.

Although we initially considered TAE for hemostasis because the patient had severe hepatic dysfunction, TAE was decided against because of a potentially increased risk of hepatic failure. The patient was therefore treated conservatively. However, bleeding continued, shock developed, and the patient required transfusion of more than 1000 mL of blood to maintain blood pressure. On the second hospital day, the anemia progressed and bleeding became difficult to control. Because the tumor was exactly 3 cm in diameter, we thought it would be possible to achieve hemostasis together with complete tumor necrosis with minimal damage to the surrounding hepatic parenchyma if the lesion could be thermocoagulated with 1 application of RFA. Contrast sonography (Sonoline Elegra; Siemens AG, Erlangen, Germany) was used to localize the bleeding site. Because a vascular signal could not be detected with conventional power Doppler imaging of the S2 lesion, 2.5 g of the contrast agent Levovist (SH U 508A; Schering AG, Berlin, Germany) was administered by bolus intravenous injection, and sonography was performed with contrast harmonic (gray scale B-mode) imaging. During the early phase, real-time observation of leakage of microbubbles from the tumor surface confirmed the diagnosis of ruptured HCC (Figure 2). After obtaining informed consent, we performed RFA (Cool-Tip radio frequency system; Radionics, Burlington, MA) of the bleeding lesion under sonographic guidance on the same day (Figure 3). The tumor was pierced with a 3-cm electrode needle, and RFA was performed for 12 minutes. Immediately after RFA, contrast harmonic imaging was repeated, confirming no tumor blood flow and no leakage of the contrast agent into the peritoneum (Figure 4). After the procedure, blood pressure stabilized and anemia did not progress. No complications occurred. Liver function also improved, and the postprocedure course was initially good. However, hepatic failure progressed 1 month after the procedure, and the patient died on the 60th hospital day.

Figure 2. Abdominal contrast sonography. **A**, The 3-cm tumor is visible on the S2 liver surface (large arrow). During the early phase, the contrast agent flowed into the tumor, and leakage of microbubbles from the tumor surface into the peritoneum was observed (small arrows). The diagnosis of ruptured HCC was thereby confirmed. **B**, The HCC tumor (large arrow) shows uniform contrast enhancement.

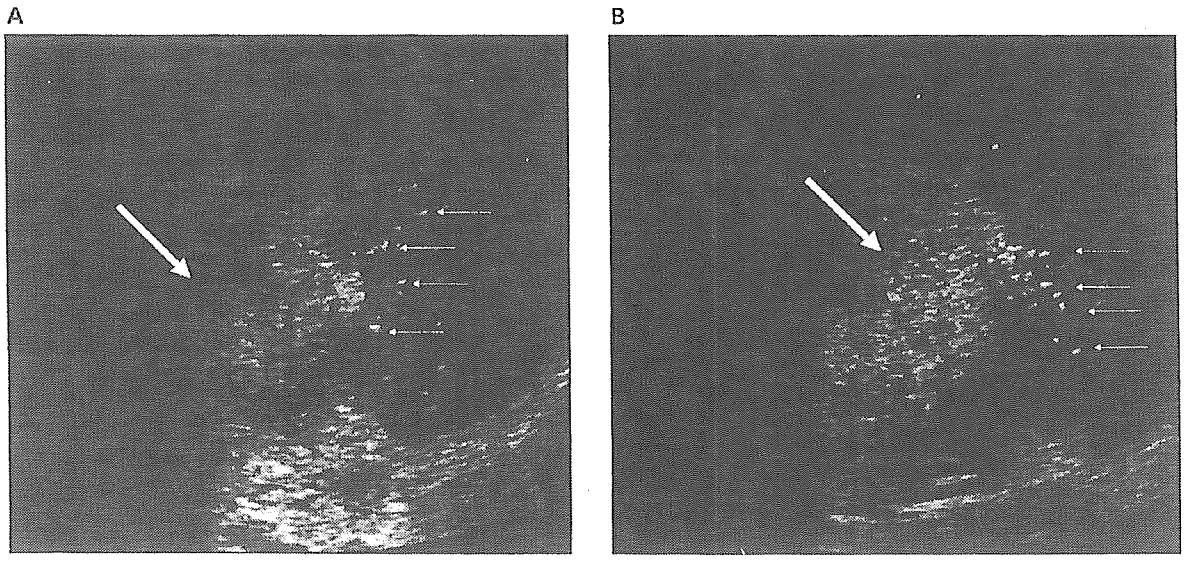

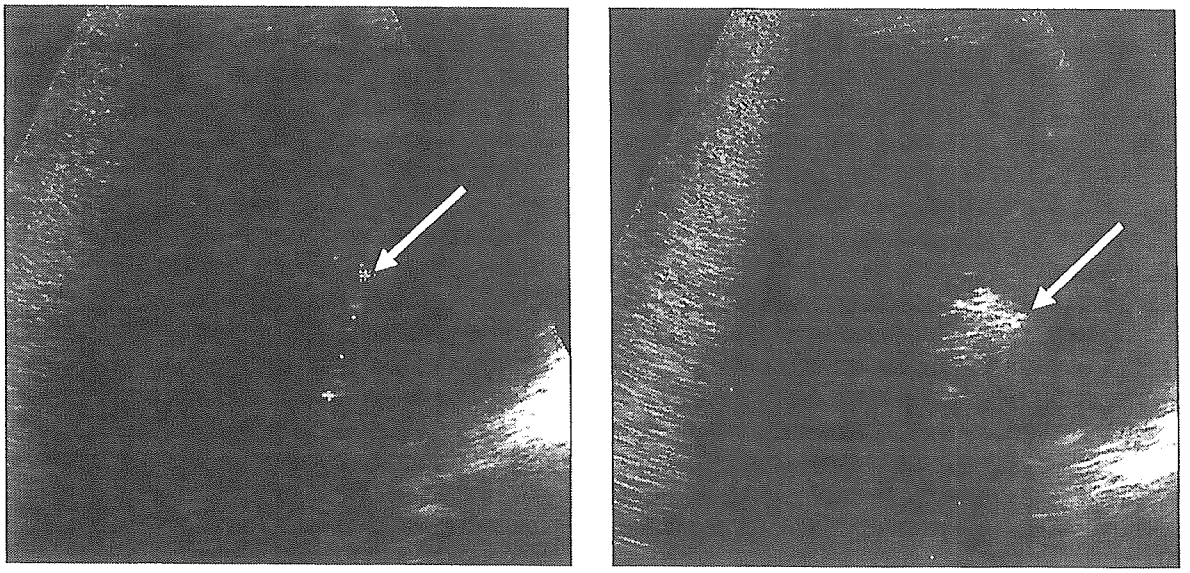

A B

Figure 3. Sonographically guided RFA for ruptured HCC. **A**, The RFA electrode needle was inserted into the tumor along with the puncture guideline (arrow). **B**, After RFA, the entire tumor became strongly echoic (arrow).

Discussion

In ruptured HCC, imaging findings suggestive of blood within the peritoneum include hyperdense areas within the ascites on CT scanning and floating hyperechoic areas (corresponding to blood clots) on sonography. Leakage of contrast medium on contrast CT helps confirm the diagnosis, but localizing the bleeding site is often difficult. Even on angiography, the diagnostic rate is less than 20% based on extravascular leakage of contrast medium.[1] In a study of color Doppler sonography performed to identify the site of bleeding in ruptured HCC, Ishida et al[6] reported that jet color flow imaging was useful in delineating the surface of the ruptured tumor. However, all the ruptured tumors were in the right hepatic lobe, so the usefulness of this procedure for tumors in the left hepatic lobe, which is subject to a cardiac apical motion artifact, could not be evaluated.

Figure 4. Contrast sonography after RFA. **A**, On contrast sonography after RFA, no blood flow into the tumor was observed during the early phase (arrow). **B**, During the late phase, the tumor appeared as a defect (arrow). There was no leakage of contrast into the peritoneum during either phase, thus confirming hemostasis.

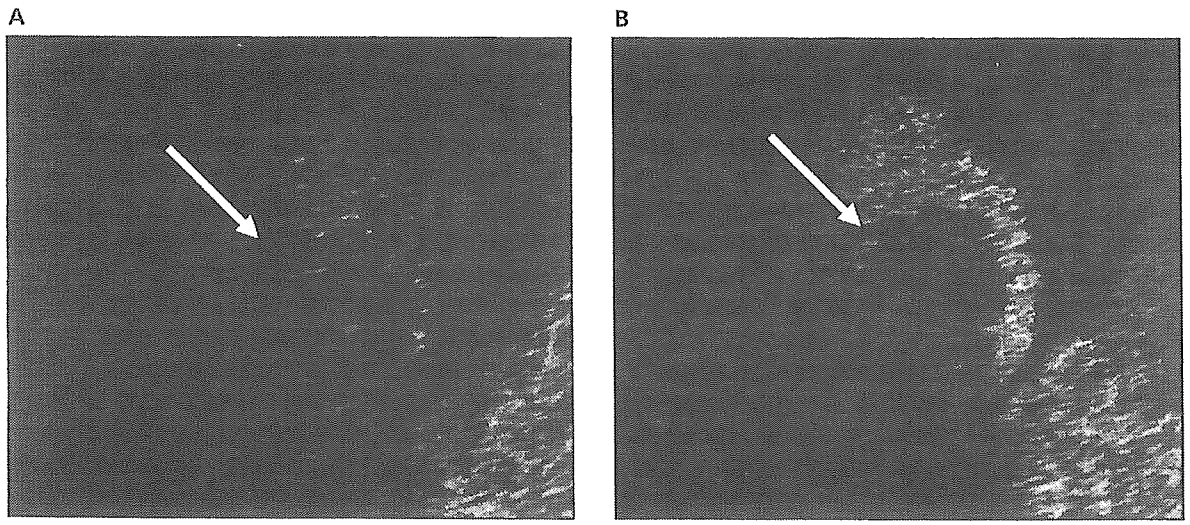

A B

In the case reported here, the ruptured tumor was in the left hepatic lobe. However, the blood flow signal from the tumor surface could not be identified on color flow imaging, perhaps because of the decreased sensitivity that was used to avoid a motion artifact from the cardiac apex. We were able to localize the site of bleeding by using contrast harmonic imaging. Compared with conventional color Doppler imaging, contrast harmonic imaging is highly sensitive in the detection of blood flow and can identify bleeding sites even when only slight bleeding is present. The disadvantage of contrast sonography is attenuation of contrast effects in deeper areas. In our patient, however, the ruptured tumor was on the liver surface, and imaging could be performed under conditions of optimal sensitivity in the presence of ascites. In addition, the use of an intravenous sonographic contrast agent is safer than iodine contrast material. Hence, contrast harmonic imaging is useful because it can be repeated to evaluate the effects of treatment immediately after hemostasis. A literature search revealed only 1 other report of ruptured HCC in which extravascular leakage of contrast material was observed in real time with the use of an intravenous sonographic contrast agent.[7] In that study, contrast color Doppler imaging was used, whereas in our study, we used contrast harmonic imaging. In comparison with conventional Doppler imaging, contrast harmonic imaging provides higher resolution because it is not affected by motion artifacts or blooming. Indeed, we were able to clearly observe extravascular leakage of each microbubble in our case. In addition, because contrast harmonic imaging is a gray scale B-mode technique, it is easier to perform percutaneous local ablative procedures under contrast guidance than with color Doppler imaging.

Very few reports have discussed control of bleeding in ruptured HCC with the use of percutaneous local ablation procedures such as PEIT and percutaneous microwave coagulation therapy. One reason is because accurate localization of the site of bleeding is difficult with conventional sonography. However, identification of the bleeding site with contrast harmonic sonography permits a percutaneous approach to the tumor, allowing hemostasis to be achieved with local ablative therapy. Radio frequency ablation is a novel procedure that allows thermocoagulation of a 3-cm lesion during a single procedure. For lesions 3 cm or less in diameter, RFA yields a high local cure rate, a less than 5% local recurrence rate, and a low incidence of posttreatment complications, including death.[8] We could only find 3 other case reports in which RFA was used, as in our patient, to control bleeding due to ruptured HCC.[9–11] Two of these cases were refractory to initial hemostatic treatment with TAE, and the remaining case was treated with RFA alone, although the site of bleeding was not identified. In each of these cases, hemostasis was achieved with a single procedure, without serious complications. One of the limitations of RFA is a cooling effect near large vessels and potential injury to bile ducts.[12] Because of this cooling effect, hemostasis with RFA may be insufficient in cases of extensive bleeding. However, contrast harmonic imaging is repeated immediately after the procedure, so even if hemostasis is incomplete, another method to control the bleeding such as PEIT or percutaneous microwave coagulo-necrotic therapy can be selected. Moreover, for ruptured HCC on the hepatic surface, the risk of bile duct injury is low. In addition, in the presence of intraperitoneal bleeding, an ample space forms between the liver surface and the skin, abdominal wall, diaphragm, and bowel. Therefore, the risk of complications due to thermal injury is low; as a result, RFA can be considered a safe procedure.

By the time our patient arrived at the hospital, secondary hepatocyte necrosis due to hemorrhage had already occurred. The development of delayed hepatic failure and subsequent limited survival may have resulted from hemostasis being performed long after the onset of tumor rupture. Ruptured HCC is generally associated with a poor prognosis, but prompt control of bleeding may permit radical treatment, prevent progression of hepatic failure, and improve the prognosis. Radio frequency ablation is useful for both hemostasis and radical cure. Furthermore, when compared with hepatectomy, RFA is minimally invasive and thus minimizes loss of the surrounding hepatic parenchyma.

In conclusion, the combination of contrast harmonic sonography and RFA enabled bedside diagnosis, hemostasis, and radical treatment of ruptured HCC. This case suggests that the procedure might become quite valuable and well worth trying, at least as a palliative treatment of ruptured HCC. Further studies are needed to elucidate indications for such treatment.

References

1. Liver Cancer Study Group of Japan. Primary liver cancer in Japan: clinicopathological features and results of surgical treatment. Ann Surg 1990; 211:277–287.
2. Yeh CN, Lee WC, Jeng LB, Chen MF, Yu MC. Spontaneous tumour rupture and prognosis in patients with hepatocellular carcinoma. Br J Surg. 2002; 89:1125–1129.
3. Marini P, Vilgarin V, Belghiti J. Management of spontaneous rupture of liver tumors. Dig Surg 2002; 19:109–113.
4. Miyamoto M, Sudo T, Kuyama T. Spontaneous rupture of hepatocellular carcinoma: a review of 172 Japanese cases. Am J Gastroenterol 1991; 86:67–71.
5. Uchida K, Nakata S, Iwase H, Yamamoto H, Kasahara H, Konagaya T. Imaging diagnosis of ruptured site in hepatocellular carcinoma [in Japanese]. Nippon Shokakibyo Gakkai Zasshi 1989; 86:1287–1291.
6. Ishida H, Konno K, Hamashima Y, et al. Sonographic and color Doppler findings of rupture of liver tumors. Abdom Imaging 1998; 23:587–591.
7. Chou YH, Chiou HJ, Tiu CM, Chen JD, Hung GS, Chiang JH. Some unusual complications of malignancies, case 1: spontaneous rupture of hepatocellular carcinoma demonstrated by contrast-enhanced sonography. J Clin Oncol 2002; 20:4108–4111.
8. Curley SA, Izzo F, Ellis LM, Nicolas Vauthey J, Vallone P. Radiofrequency ablation of hepatocellular cancer in 110 patients with cirrhosis. Ann Surg 2000; 232:381–391.
9. Ng KK, Lam CM, Poon RT, Law WL, Seto CL, Fan ST. Radiofrequency ablation as a salvage procedure for ruptured hepatocellular carcinoma. Hepatogastroenterology 2003; 50:1641–1643.
10. Kobayashi M, Ikeda K, Hosaka T, et al. Successful control of ruptured hepatocellular carcinoma with radiofrequency ablation. J Gastroenterol 2004; 39:192–193.
11. Fuchizaki U, Miyamori H, Kitagawa S, Kaneko S. Radiofrequency ablation for life-threatening ruptured hepatocellular carcinoma. J Hepatol 2004; 40:354–355.
12. Wood TF, Rose DM, Chung M, Allegra DP, Foshag LJ, Bilchik AJ. Radiofrequency ablation of 231 unresectable hepatic tumors: indications, limitations, and complications. Ann Surg Oncol 2000; 7:593–600.

Available online at www.sciencedirect.com
SCIENCE DIRECT®
ELSEVIER
Biochemical and Biophysical Research Communications 334 (2005) 606–612
BBRC
www.elsevier.com/locate/ybbrc

Inhibitory effect of etodolac, a selective cyclooxygenase-2 inhibitor, on stomach carcinogenesis in *Helicobacter pylori*-infected Mongolian gerbils

Hirohito Magari [a], Yasuhito Shimizu [a], Ken-ichi Inada [c], Shotaro Enomoto [a], Tatsuji Tomeki [a], Kimihiko Yanaoka [a], Hideyuki Tamai [a], Kenji Arii [a], Hiroya Nakata [a], Masashi Oka [a], Hirotoshi Utsunomiya [b], Yutaka Tsutsumi [c], Tetsuya Tsukamoto [d], Masae Tatematsu [d], Masao Ichinose [a,*]

[a] *Second Department of Internal Medicine, Wakayama Medical University, 811-1 Kimiidera, Wakayama-City, Wakayama 641-0012, Japan*
[b] *Department of Pathology, Wakayama Medical University, 811-1 Kimiidera, Wakayama-City, Wakayama 641-0012, Japan*
[c] *First Department of Pathology, Fujita Health University School of Medicine, Toyoake, Aichi 470-1192, Japan*
[d] *Laboratory of Pathology, Aichi Cancer Center Research Institute, Aichi 464-8681, Japan*

Received 13 June 2005
Available online 1 July 2005

Abstract

The effect of the selective COX-2 inhibitor, etodolac, on *Helicobacter pylori* (*Hp*)-associated stomach carcinogenesis was investigated in Mongolian gerbils (MGs). *Hp*-infected MGs were fed for 23 weeks with drinking water containing 10 ppm *N*-methyl-*N*-nitrosourea. They were then switched to distilled water and placed on a diet containing 5–30 mg/kg/day etodolac for 30 weeks. We found that etodolac dose-dependently inhibited the development of gastric cancer, and no cancer was detected at a dose of 30 mg/kg/day. Etodolac did not affect the extent of inflammatory cell infiltration or oxidative DNA damage, but it significantly inhibited mucosal cell proliferation and dose-dependently repressed the development of intestinal metaplasia in the stomachs of *Hp*-infected MGs. These results suggest that COX-2 is a key molecule in inflammation-mediated stomach carcinogenesis and that chemoprevention of stomach cancer should be possible by controlling COX-2 expression or activity.
© 2005 Elsevier Inc. All rights reserved.

Keywords: Stomach cancer; COX-2; *Helicobacter pylori*; Mongolian gerbils; Chemoprevention; Etodolac; Carcinogenesis

Despite a recent decline in its incidence, gastric cancer remains one of the most common malignancies in the world. Its pathogenesis is known to be closely associated with several environmental factors, including a high intake of salted foods and nitrates, and insufficient intake of fresh fruits and vegetables [1–6]. Clinicopathological and histological studies suggest a correlation between chronic atrophic gastritis (CAG) and the development of gastric cancer [1,7]. Moreover, since the discovery of *Helicobacter pylori* (*Hp*) in 1983, considerable evidence has accumulated for its involvement in CAG. *Hp* colonizes the stomach mucosa and triggers a series of inflammatory reactions [8,9], and it is now considered to be the most important cause and a potent driving force for subsequent progression of CAG.

Chronic atrophic gastritis is the first step in the series of events leading to carcinogenesis of the stomach, a process referred to as the CAG-metaplasia-dysplasia-cancer sequence [1,7]. By following up 4655 healthy asymptomatic males for a mean period of 7.7 years, we recently found that the risk of developing gastric cancer increases in a step-wise manner with the progression

* Corresponding author. Fax: +81 734 45 3616.
E-mail address: ichinose@wakayama-med.ac.jp (M. Ichinose).

0006-291X/$ - see front matter © 2005 Elsevier Inc. All rights reserved.
doi:10.1016/j.bbrc.2005.06.132

of CAG, and the cancer incidence rate reached a maximal level of 871 per 100,000 person-years in individuals with metaplastic gastritis [10]. Because gastric cancer did not develop in *Hp*-free subjects during the study period, it appears that *Hp*-associated gastritis is central in the Japanese carcinogenic pathway.

Meanwhile, elevated expression of cyclooxygenase 2 (COX-2), a prostaglandin-synthesizing enzyme, is observed in a wide variety of human malignancies, including gastric cancer [11–14]. Various in vitro and in vivo studies strongly suggest that COX-2 is involved in a major early oncogenic event in various human malignancies. In addition, epidemiological and preclinical animal studies indicate that regular intake of either nonselective or selective COX-2 inhibitors reduces the risk of several forms of human cancer [15–17]. Thus, it is conceivable that targeted inhibition of abnormally or improperly elevated COX-2 will be a highly effective strategy for preventing these epithelial malignancies.

The current model for human stomach carcinogenesis emphasizes the importance of *Hp* infection. *Hp*-induced chronic gastritis increases the level of COX-2 expression in the stomach mucosa [18–20]. Enhanced expression of COX-2 is also observed in intestinal metaplasia, dysplasia, and gastric adenoma, which are considered precancerous lesions [11,21]. Thus, it is likely that the development of cancer can be reduced by regulating COX-2 expression or activity. The selective COX-2 inhibitor, Celecoxib, has been reported to prevent *N'*-methyl-*N'*-nitro-*N*-nitrosoguanidine-induced chemical carcinogenesis in the rat [22]. Furthermore, while we were preparing this manuscript, Nam et al. [23] reported that another selective COX-2 inhibitor, nimesulide, represses the development of gastric cancer in *Hp*-infected C57/BL6 mice. In this mouse model, however, *Hp*-associated gastritis is mild and cancer development does not follow the characteristic series of events seen in humans [9,24]. The response of Mongolian gerbils (MGs) to infection with *Hp*, in contrast, is quite similar to that in humans: as in humans, *Hp* causes severe and persistent infection in the stomach of MGs; induces a similar series of pathological events, including the development of chronic active gastritis, peptic ulcers, intestinal metaplasia; and results in the same histological types of gastric cancer. These pathological events are not observed in any other animal model [25–27]. Thus, MGs are considered to be the best experimental model for human stomach carcinogenesis. Therefore, in the present study, we investigated the effect of a selective COX-2 inhibitor, etodolac, on *Hp*-associated stomach carcinogenesis in MGs.

Materials and methods

Chemicals. *N*-Methyl-*N*-nitrosourea (MNU; Wako Pure Chemical Industries, Tokyo, Japan) was freshly prepared at 10 ppm in distilled water twice a week. The MGs were fed the solution ad libitum as drinking water from light-shielded bottles. The stock diet was made up by mixing various amounts of etodolac (kindly provided by Nippon Shinyaku, Kyoto, Japan) with CRF-1 (Oriental Yeast, Tokyo, Japan) so that daily intake of etodolac would be 5, 10, or 30 mg/kg/day.

Bacteria. *Hp* samples (Type I Strain ATCC 43504; American Type Culture Collection, Rockville, MD) containing approximately 3.0×10^8 colony forming units per milliliter were used as the inoculum. After a 24-h fast, samples (1 ml) were delivered intragastrically (i.g.) using an oral catheter. Vehicle alone (Brucella broth) was administered i.g. as a control.

Animals. Specific pathogen-free 6-week-old male MGs (*Meriones unguiculatus*; MGS/Sea; Seac Yoshitomi, Fukuoka, Japan) were housed in steel cages with hardwood chip bedding in an air-conditioned biohazard room with a 12-h light/12-h dark cycle. The animals were fed γ-irradiated (30 kGy) stock diet.

Experimental design. The experimental design was approved by the Animal Research Committee of Wakayama Medical University. As shown in Fig. 1, a total of 154 gerbils were divided into five groups (A–E). Animals were inoculated with *Hp* (groups A–D; $n = 28$, 35, 35, and 40, respectively) or vehicle (Brucella broth) alone (group E; $n = 16$). After 1 week, groups A–D were given MNU in the drinking water at a concentration of 10 ppm. MNU was not administered to group E. After 23 weeks, all groups were switched to autoclaved distilled water as drinking water. In groups B–D, the animals were given the stock etodolac diet from week 24 until week 53, whereas the animals in groups A and E received the control diet. The daily administered dosage of etodolac was 0 mg/kg/day in groups A and E, 5 mg/kg/day in group B, 10 mg/kg/day in group C, and 30 mg/kg/day in group D. On the 53rd experimental week, the animals were fasted for 24 h, placed under deep ether anesthesia, and subjected to laparotomy with excision of the stomach. One small segment of this stomach tissue was stored at −80 °C immediately after resection for isolation of total RNA. The remainder was used for histological examination.

Tissue preparation and histological examination. The excised stomachs were fixed in 10% neutral-buffered formalin and embedded in paraffin. Tissues sections (5 μm) were stained with haematoxylin–eosin (H&E) and were analyzed by immunohistochemistry with anti-*Hp* serum (Dako, Glostrup, Denmark), anti-COX-2 serum (Santa Cruz Biotechnology, Santa Cruz, CA), or anti-proliferating cell nuclear antigen (PCNA) serum (Dako). Histological features of mucosal inflammation and intestinal metaplasia were evaluated for each specimen under a light microscope. The degree of inflammatory cell infil-

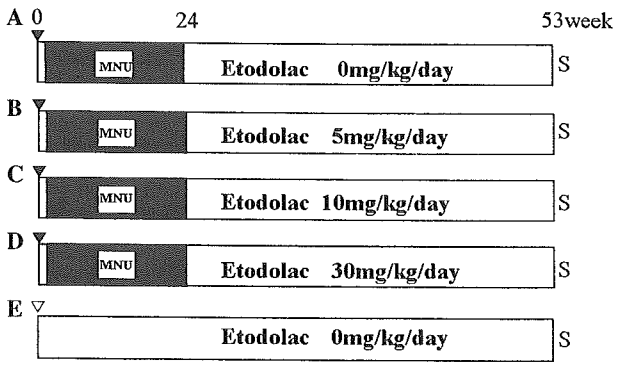

Fig. 1. Protocol of the animal experiment. At the beginning of the experiment, animals were inoculated i.g. with *Hp* (groups A–D; ▼) or vehicle (Brucella broth; group E; ▽). After 1 week and until 23 weeks, the animals were given drinking water containing no (group E; open bars) or 10 ppm MNU (groups A–D; filled bars). All groups were then switched to distilled water and given a diet containing no drug (groups A and E) or 5 (group B), 10 (group C), or 30 (group D) mg/kg/day etodolac. The animals were sacrificed (S) on week 53.

tration and the area of intestinal metaplasia were scored as follows: 0, normal; 1, mild; 2, moderate; 3, marked. For the evaluation of mucosal cell proliferation, the proportion of PCNA-positive cells per 1000 mucosal cells was assessed in the antrum and corpus as described previously [28].

Isolation of total RNA and quantitative reverse transcription-polymerase chain reaction. Total RNA was isolated using Trizol reagent (Life Technologies, Gaithersburg, MD) from the frozen stomach segments, and cDNA synthesis was carried out using 1 μg of total RNA and a First Strand cDNA Synthesis Kit for reverse transcription-polymerase chain reaction (RT-PCR) (AMV) (Roche, Indianapolis, IN). PCR was performed with a LightCycler (Roche Diagnostics, Mannheim, Germany), with glyceraldehyde 3-phosphate dehydrogenase (GAPDH) as a reference. Primers for COX-2 and GAPDH were designed based on their cDNA sequences (GenBank Accession Nos. AB044784 and AB040445, respectively). PCR was carried out with an initial denaturation at 95 °C for 10 min, followed by 45 cycles of 95 °C for 10 s, 60 °C for 10 s, and 72 °C for 16 s. LightCycler software, version 3.5 (Roche Diagnostics) was used to determine the amount of mRNA from each sample.

Serum levels of anti-Hp antibodies and 8-hydroxy-2′-deoxyguanosine (8-OHdG). Blood samples from each animal were centrifuged and separated sera were stored at −80 °C until use. The anti-*Hp* IgG level was measured in the serum using an enzyme-linked immunosorbent assay (ELISA) (Seac Yoshitomi) with peroxidase-conjugated anti-mouse immunoglobulin as the secondary antibody. Optical density at 450 nm (OD_{450}) was measured spectrophotometrically. A cut-off value of 0.1 was used as an indicator of Hp infection [25]. These sera were also centrifuged at 10,000*g* for 30 min at 4 °C through centrifugal filter devices (Microcon YM-10, Millipore, Bedford, MA) and used for the measurement of 8-OHdG by ELISA (high sensitive 8-OHdG check; Japan Institute for the Control of Aging, Shizuoka, Japan).

Statistical analyses. An unpaired *t* test or a Mann–Whitney *U* test was applied to determine the significance of differences between two groups. Survival curves of the animals were calculated by the Kaplan–Meier method and the differences were evaluated using a log-rank test. The incidence of cancer was assessed using Fisher's exact probability method. *P* values <0.05 were considered to be statistically significant.

Results

In the present study, we investigated whether long-term treatment with etodolac, a selective COX-2 inhibitor, can be used to prevent *Hp*-associated stomach carcinogenesis. The animals were separated into five groups: groups A–D were *Hp-infected* and were divided according to the dose of drug administration, and group E (control group) was neither infected with *Hp* nor treated with etodolac (Fig. 1). During the 53-week experimental period, the body weight gain of group C (10 mg/kg/day etodolac) was significantly less than group E (control), but there was no significant difference in the food intake or body weight gain among the other experimental groups of the animals. Also, a significant difference was not observed in the appearance or survival rates among the various groups.

In all of the *Hp*-infected animals (groups A–D), marked infiltration of inflammatory cells was observed in the lamina propria and submucosa. This infiltration was predominantly lymphocytes, although some macrophages and neutrophils were also observed. The histological examination also revealed hyperplasia of the epithelia together with erosions, lymphoid follicle formation, and intestinal metaplasia. These results are consistent with our previous findings [29]. COX-2 expression, which was not observed in the stomach of non-infected animals, was also induced by *Hp* infection. Immunohistochemistry with a specific anti-COX-2 antibody showed that a considerable number of mesenchymal cells and infiltrating mononuclear cells became COX-2-positive in the *Hp*-infected stomach (not shown).

Etodolac treatment did not have significant influence on the number of COX-2-expressing mesenchymal or inflammatory cells in the stomach, but the intensity of the staining was significantly reduced. The mucosal level of COX-2 mRNA expression tended to be dose-dependently reduced by etodolac treatment. However, the difference in the COX-2 mRNA level between groups with and without etodolac treatment was not significant (Fig. 2). This is probably due to the fact that RNA from COX-2 expressing cells represents a relatively small proportion of the total mucosal RNA.

The number of inflammatory cells infiltrating the *Hp*-infected stomach did not appear to be influenced by etodolac treatment because there was no significant difference in the inflammatory scores among the etodolac-treated groups (Fig. 3A). Infection with *Hp* remarkably elevated the serum level of 8-OHdG, a biomarker of oxidative DNA damage, but it was not significantly reduced by etodolac treatment, which suggests that etodolac did not reduce inflammation-mediated mucosal cell damage (not shown). In contrast, we found that the etodolac treatment dose-dependently reduced the serum

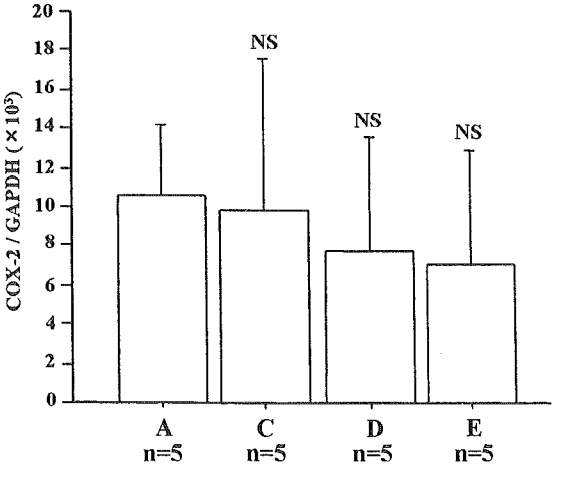

Fig. 2. Effect of etodolac on the mucosal level of COX-2 mRNA expression in *Hp*-infected MG stomach. Total RNA was isolated from *Hp*-infected MG stomach mucosa and used to generate cDNA. PCR was performed using specific primers for COX-2 and GAPDH, and the level of COX-2 mRNA in each sample was determined using LightCycler software. NS, not significant vs. group A.

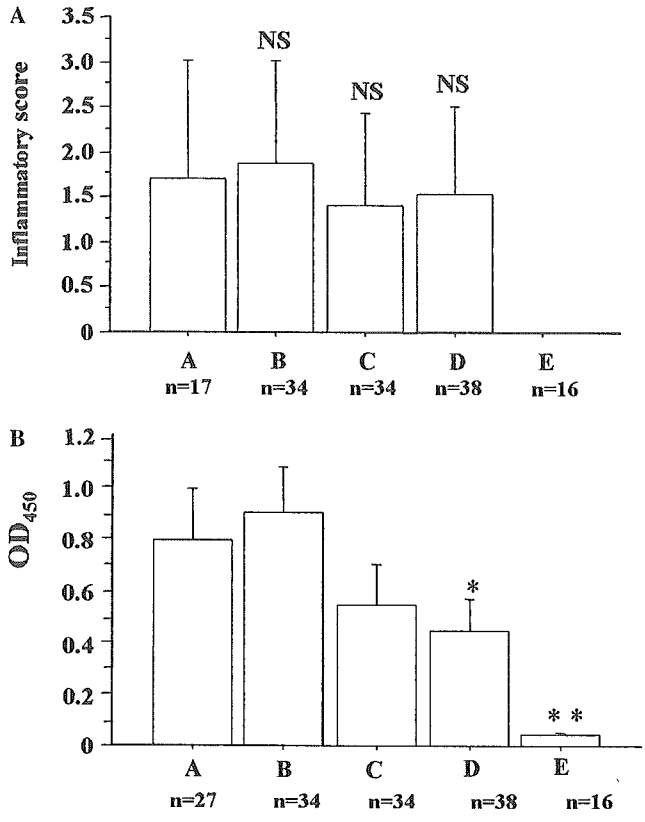

Fig. 3. Effect of etodolac on: (A) the number of inflammatory cells infiltrating the stomach mucosa and (B) the serum level of anti-*Hp* antibodies in *Hp*-infected MGs. (A) The degree of inflammatory cell infiltration was scored as follows: 0, normal; 1, mild; 2, moderate; 3, marked. NS, not significant vs. group A. (B) The anti-*Hp* IgG levels in serum were measured by ELISA. An $OD_{450} > 0.1$ was used to confirm infection by *Hp*. $^{*}p < 0.05$ vs. group B; $^{**}p < 0.01$ vs. groups A–D.

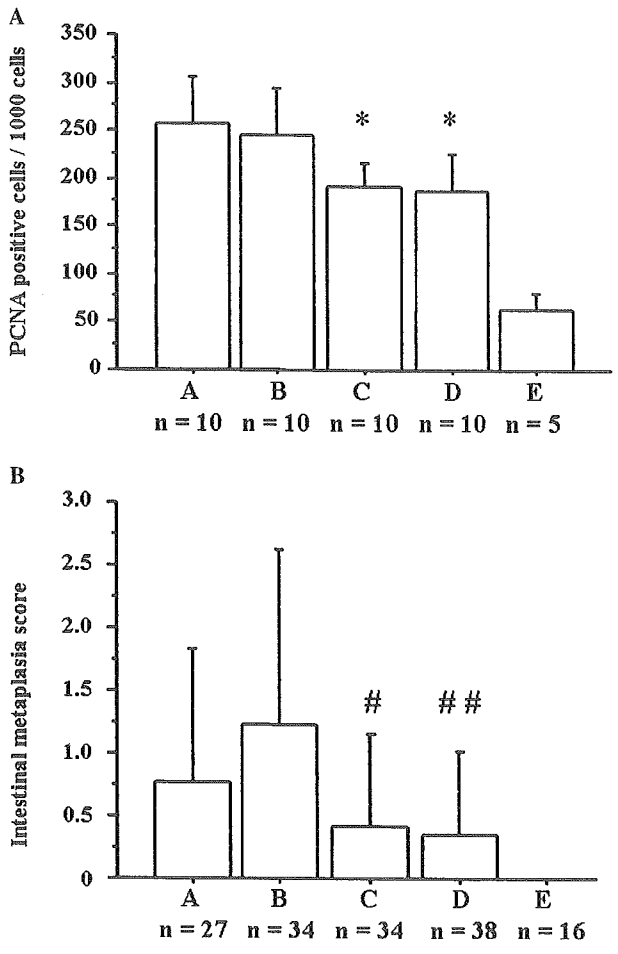

Fig. 4. Effect of etodolac on: (A) the proliferation of mucosal cells and (B) the development of intestinal metaplasia in the stomachs of *Hp*-infected MGs. (A) Anti-PCNA immunohistochemistry was used to evaluate mucosal cell proliferation. The proportion of PCNA-positive cells per 1000 mucosal cells was determined in each experiment. $^{*}p < 0.01$ vs. groups A and B. (B) The extent of intestinal metaplasia in each experimental group was scored as described as follows: 0, normal; 1, mild; 2, moderate; 3, marked. $^{\#}p < 0.05$ vs. group B; $^{\#\#}p < 0.01$ vs. group B.

level of anti-*Hp* antibodies, with a statistically significant reduction at 30 mg/kg/day (group D) (Fig. 3B).

Infection with *Hp* greatly enhanced mucosal cell proliferation as revealed by anti-PCNA immunohistochemistry (Fig. 4A). Etodolac treatment resulted in a step-wise and significant reduction in the proliferation of *Hp*-infected mucosal cells ($p < 0.01$). In addition, etodolac repressed the development of intestinal metaplasia, an end result of persistent gastritis (Fig. 4B). These metaplastic changes were significantly reduced in the groups C and D which were administered higher doses of etodolac.

Finally, we examined the incidence and development of cancer in the infected animals at the end of the experimental period. Cancers were mostly observed in the pyloric mucosa adjacent to the fundic region. As shown in Fig. 5, a majority of them were well-differentiated adenocarcinomas, although we also observed the development of signet-ring cell carcinoma. The incidence of cancer in the experimental groups is shown in Table 1. As a result of long-lasting infection with *Hp*, 14.8% of the animals in group A developed cancer. The cancer incidence in the group treated with a low dose of etodolac (group B) was higher than the control group, but the difference was not significant. The incidence of cancer decreased in a step-wise manner with the dose of etodolac, and the development of the cancer was completely inhibited at a dose of 30 mg/kg/day (group D).

Discussion

In the present study, etodolac, a selective inhibitor of COX-2, dose-dependently inhibited the development of gastric cancer in the mucosa of *Hp*-infected MGs. The effect of etodolac was so strong that no cancer developed in MGs treated with 30 mg/kg/day. This is the first demonstration that a selective COX-2 inhibitor can prevent stomach carcinogenesis in the CAG-metaplasia-cancer sequence.

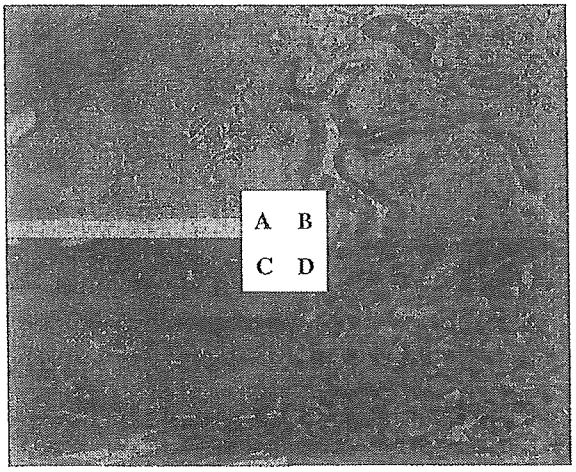

Fig. 5. Typical adenocarcinoma in the pyloric mucosa of *Hp*-infected MGs. Shown are a typical well-differentiated adenocarcinoma (A,B) and a signet-ring cell carcinoma (C,D) stained with H&E. Images were obtained at 100× (A,C) and 400× (B,D).

The basic mechanism for the observed inhibitory effect of etodolac remains unclear, but our current findings agree with epidemiological studies showing that aspirin and other non-steroidal anti-inflammatory drugs, which are non-selective COX inhibitors, reduce the risk for gastric cancer [30–32]. We expect that etodolac acts by inhibiting the inducible form of COX-2, a key enzyme in prostaglandin biosynthesis. COX-2 is readily induced by various stimuli, including proinflammatory cytokines, growth factors, and tumor promoters. *Hp* has been shown to directly upregulate COX-2 mRNA expression in gastric mucosal cells in vitro [33]. Chronic inflammation in other organs, for example, in ulcerative colitis or hepatitis C virus-associated chronic hepatitis, is thought to play a central role in the accumulation of genetic events leading to transformation and cancer by increasing the number of target cells or by promoting the proliferation of initiated cells [34–36]. In these cases, the induction of COX-2 appears to participate in the establishment of the carcinogenic state. In the current studies, we found that etodolac inhibits mucosal cell proliferation and the development of intestinal metaplasia, a precancerous lesion caused by accumulation of genetic events in the stomach epithelia. This strongly suggests that COX-2 also participates in inflammation-mediated carcinogenesis in the *Hp*-infected stomach.

Measurement of the serum 8-OHdG level showed that etodolac did *not* cause significant differences in the extent of oxidative DNA damage. In addition, etodolac has a stronger inhibitory effect on the development of cancer than on the development of intestinal metaplasia. This suggests that the anti-carcinogenic effect of etodolac is mediated by the suppression of tumor promotion rather than initiation, and it is consistent with studies showing that the COX-2 pathway is involved in tumor promotion in several other organs [37]. The effect of etodolac on gastritis was unclear because treatment with etodolac did not result in significant difference in the inflammatory score.

Interestingly, the titers of anti-*Hp* antibodies were significantly lower in etodolac-treated animals. This is consistent with the recent hypothesis that COX-2 inhibitors reduce B cell antibody production, in part, by attenuating their differentiation to plasma cells [38]. A high antibody titer is thought to reflect severe inflammation in *Hp*-infected stomach mucosa, and its long-term persistence appears to lead to the progression of atrophic changes and intestinal metaplasia [39,40]. Indeed, in previous studies, the enhancement of carcinogenesis by *Hp* has been observed mainly in animals with a high antibody titer [29,41]. This is not surprising because a T helper-2 humoral immune response is thought to be important in the development of cancer [29]. Therefore, reduction of the humoral immune response may contribute to the anti-carcinogenic activity of etodolac.

A variety of previous studies have provided evidence that the effect of selective COX-2 inhibitor is mediated not only by selectively inhibiting COX-2 but also by modifying COX-2-independent mechanisms. For example, both non-selective and COX-2 selective inhibitors have been shown to suppress the activation of NF-κB by *Hp*. This may subsequently reduce transcription of the COX-2 gene [42]. A relatively high dose of etodolac is needed for the anti-carcinogenic effect, indicating that it may be mediated by COX-2-independent mechanisms. Further studies are required to determine how this COX-2 inhibitor prevents stomach carcinogenesis.

Table 1
Effect of etodolac on development of gastric cancer in male Mongolian gerbils

Group	Treatment	Number of tumor-bearing Mongolian gerbils (%)	No. of Mongolian gerbils	No. of cancer		
				Well	Poor	Sig
A	*Hp* + MNU + etodolac (0 mg/kg/day)	4 (14.8)*	27	3	0	1
B	*Hp* + MNU + etodolac (5 mg/kg/day)	8 (23.5)*	34	8	0	0
C	*Hp* + MNU + etodolac (10 mg/kg/day)	3 (8.8)	34	3	0	1
D	*Hp* + MNU + etodolac (30 mg/kg/day)	0 (0.0)	39	0	0	0
E	Br + etodolac (0 mg/kg/day)	0 (0.0)	16	0	0	0

Hp, *H. pylori* (i.g.); Br, Brucella broth (i.g.); Well, well-differentiated adenocarcinoma; Poor, poorly differentiated a denocarcinoma; Sig, signet-ring cell carcinoma.

* Significantly different from group D ($p < 0.05$) by Fisher's exact test.

In conclusion, the present study clearly demonstrates that etodolac potently inhibits inflammation-mediated carcinogenesis in the *Hp*-infected stomach. This effect is due to the inhibition of cell proliferation, alteration of the humoral immune response, and slowing of the CAG-metaplasia-cancer sequence. In addition, the potent anti-carcinogenic effect of etodolac strongly suggests that COX-2 plays a key role in *Hp*-associated stomach carcinogenesis, which is a main route for the development of cancer in high-risk areas throughout the world. Furthermore, it may be possible to prevent stomach cancer by chemotherapy aimed at reducing COX-2 expression. In addition to eradication of *Hp*, selective COX-2 inhibitors should provide a potent strategy for cancer prevention. However, the long-term use of other selective COX-2 inhibitors is known to be associated with an elevated risk of cardiovascular events [43–46], and etodolac is expensive and less cost-effective than therapy aimed at eradicating *Hp*. These factors must be considered before etodolac is used clinically for the chemoprevention of gastric cancer.

Our previous study revealed that subjects with extensive metaplastic gastritis have the highest risk for the development of gastric cancer (the annual cancer incidence, 0.87%). These individuals represent less than 1% of the middle-aged Japanese population [10], and they cannot be treated with therapy to eradicate *Hp* because the infection is no longer present [10]. In this small population, inhibition of COX-2 may be useful for the prevention of gastric cancer.

Acknowledgment

This work was supported by a Grant-in-Aid for Cancer Research from the Ministry of Health, Labor and Welfare of Japan.

References

[1] P. Correa, The epidemiology of gastric cancer, World J. Surg. 15 (1991) 228–234.
[2] C.S. Fuchs, R.J. Mayer, Gastric carcinoma, N. Engl. J. Med. 333 (1995) 32–41.
[3] M.J. Hill, Salt and gastric cancer, Eur. J. Cancer Prev. 7 (1998) 173–175.
[4] J. Sandor, I. Kiss, O. Farkas, I. Ember, Association between gastric cancer mortality and nitrate content of drinking water: ecological study on small area inequalities, Eur. J. Epidemiol. 17 (2001) 443–447.
[5] M. Serafini, R. Bellocco, A. Wolk, A.M. Ekstrom, Total antioxidant potential of fruit and vegetables and risk of gastric cancer, Gastroenterology 123 (2002) 985–991.
[6] P. Terry, O. Nyren, J. Yuen, Protective effect of fruits and vegetables on stomach cancer in a cohort of Swedish twins, Int. J. Cancer 76 (1998) 35–37.
[7] P. Correa, Human gastric carcinogenesis: a multistep and multifactorial process—First American Cancer Society Award Lecture on Cancer Epidemiology and Prevention, Cancer Res. 52 (1992) 6735–6740.
[8] C.P. Dooley, H. Cohen, P.L. Fitzgibbons, M. Bauer, M.D. Appleman, G.I. Perez-Perez, M.J. Blaser, Prevalence of *Helicobacter pylori* infection and histologic gastritis in asymptomatic persons, N. Engl. J. Med. 321 (1989) 1562–1566.
[9] D.A. Israel, R.M. Peek, Pathogenesis of *Helicobacter pylori*-induced gastric inflammation, Aliment. Pharmacol. Ther. 15 (2001) 1271–1290.
[10] H. Ohata, S. Kitauchi, N. Yoshimura, K. Mugitani, M. Iwane, H. Nakamura, A. Yoshikawa, K. Yanaoka, K. Arii, H. Tamai, Y. Shimizu, T. Takeshita, O. Mohara, M. Ichinose, Progression of chronic atrophic gastritis associated with *Helicobacter pylori* infection increases risk of gastric cancer, Int. J. Cancer 109 (2004) 138–143.
[11] A. Ristimaki, N. Honkanen, H. Jankala, P. Sipponen, M. Harkonen, Expression of cyclooxygenase-2 in human gastric carcinoma, Cancer Res. 57 (1997) 1276–1280.
[12] C.E. Eberhart, R.J. Coffey, A. Radhika, F.M. Giardiello, S. Ferrenbach, R.N. DuBois, Up-regulation of cyclooxygenase 2 gene expression in human colorectal adenomas and adenocarcinomas, Gastroenterology 107 (1994) 1183–1188.
[13] S.I. Mohammed, D.W. Knapp, D.G. Bostwick, R.S. Foster, K.N. Khan, J.L. Masferrer, B.M. Woerner, P.W. Snyder, A.T. Koki, Expression of cyclooxygenase-2 (COX-2) in human invasive transitional cell carcinoma (TCC) of the urinary bladder, Cancer Res. 59 (1999) 5647–5650.
[14] D. Hwang, D. Scollard, J. Byrne, E. Levine, Expression of cyclooxygenase-1 and cyclooxygenase-2 in human breast cancer, J. Natl. Cancer Inst. 90 (1998) 455–460.
[15] E. Giovannucci, K.M. Egan, D.J. Hunter, M.J. Stampfer, G.A. Colditz, W.C. Willett, F.E. Speizer, Aspirin and the risk of colorectal cancer in women, N. Engl. J. Med. 333 (1995) 609–614.
[16] C.J. Grubbs, R.A. Lubet, A.T. Koki, K.M. Leahy, J.L. Masferrer, V.E. Steele, G.J. Kelloff, D.L. Hill, K. Seibert, Celecoxib inhibits *N*-butyl-*N*-(4-hydroxybutyl)-nitrosamine-induced urinary bladder cancers in male B6D2F1 mice and female Fischer-344 rats, Cancer Res. 60 (2000) 5599–5602.
[17] G. Steinbach, P.M. Lynch, R.K. Phillips, M.H. Wallace, E. Hawk, G.B. Gordon, N. Wakabayashi, B. Saunders, Y. Shen, T. Fujimura, L.K. Su, B. Levin B, The effect of celecoxib, a cyclooxygenase-2 inhibitor, in familial adenomatous polyposis, N. Engl. J. Med. 342 (2000) 1946–1952.
[18] F.K. Chan, K.F. To, Y.P. Ng, T.L. Lee, A.S. Cheng, W.K. Leung, J.J. Sung, Expression and cellular localization of COX-1 and -2 in *Helicobacter pylori* gastritis, Aliment. Pharmacol. Ther. 15 (2001) 187–193.
[19] P. Loogna, L. Franzen, P. Sipponen, L. Domellof, Cyclooxygenase-2 and Bcl-2 expression in the stomach mucosa of Wistar rats exposed to *Helicobacter pylori*, *N'*-methyl-*N'*-nitro-*N*-nitrosoguanidine and bile, Virchows Arch. 441 (2002) 77–84.
[20] L.M. Jackson, K.C. Wu, Y.R. Mahida, D. Jenkins, C.J. Hawkey, Cyclooxygenase (COX) 1 and 2 in normal, inflamed, and ulcerated human gastric mucosa, Gut 47 (2000) 762–770.
[21] J.J. Sung, W.K. Leung, M.Y. Go, K.F. To, A.S. Cheng, E.K. Ng, F.K. Chan, Cyclooxygenase-2 expression in *Helicobacter pylori*-associated premalignant and malignant gastric lesions, Am. J. Pathol. 157 (2000) 729–735.
[22] P.J. Hu, J. Yu, Z.R. Zeng, W.K. Leung, H.L. Lin, B.D. Tang, A.H. Bai, J.J. Sung, Chemoprevention of gastric cancer by celecoxib in rats, Gut 53 (2004) 195–200.
[23] K.T. Nam, K.B. Hahm, S.Y. Oh, M. Yeo, S.U. Han, B. Ahn, Y.B. Kim, J.S. Kang, D.D. Jang, K.H. Yang, D.Y. Kim, The selective cyclooxygenase-2 inhibitor nimesulide prevents *Helicobacter pylori*-associated gastric cancer development in a mouse model, Clin. Cancer Res. 10 (2004) 8105–8113.